

# Mining Intrinsic Rewards from LLM Hidden States for Efficient Best-of-N Sampling

Jizhou Guo

Zhiyuan College, Shanghai Jiao Tong University  
Shanghai, China  
sjtu18640985163@sjtu.edu.cn

Hanchen Yang

University of Illinois Chicago  
Chicago, IL, USA  
neoyang@tongji.edu.cn

Zhaomin Wu

National University of Singapore  
Singapore, Singapore  
zhaomin@nus.edu.sg

Philip S. Yu

University of Illinois Chicago  
Chicago, IL, USA  
psyu@uic.edu

## Abstract

Enhancing Large Language Model (LLM)’s performance with best-of-N sampling is effective and has attracted significant attention. However, it is computationally prohibitive due to massive, data-hungry text-based reward models. By changing the data source from text to hidden states, we introduce SWIFT (Simple Weighted Intrinsic Feedback Technique), a novel, lightweight technique that leverages the rich information embedded in LLM hidden states to address these issues, which operates on token-level and consists of only linear layers. Extensive experiments show that SWIFT outperforms baselines with less than 0.005% of the parameters of baselines, requiring only a few samples for training, demonstrating significant efficiency improvement. SWIFT’s robust scalability, applicability to some closed-source models via logits, and ability to be combined with traditional reward models to yield further performance gains underscore its practical value.

## CCS Concepts

• **Computing methodologies** → **Knowledge representation and reasoning; Natural language processing; Learning from implicit feedback; Learning latent representations.**

## Keywords

Large Language Models, Knowledge Discovery, Reward Modeling

### ACM Reference Format:

Jizhou Guo, Zhaomin Wu, Hanchen Yang, and Philip S. Yu. 2018. Mining Intrinsic Rewards from LLM Hidden States for Efficient Best-of-N Sampling. In *Proceedings of (Conference acronym 'XX)*. ACM, New York, NY, USA, 28 pages. <https://doi.org/XXXXXXX.XXXXXXX>

## 1 Introduction

The proliferation of large language models (LLMs) has unlocked unprecedented capabilities in various domains, significantly boosting

both reasoning ability and user assistance [30, 45, 62]. Best-of-N sampling, generating candidate responses and selecting response with the highest score given by a reward model, has been highlighted the potential of enhancing capabilities of LLMs [47].

Current methods generally rely on predicting reward scores based on the LLM’s generated text using independently trained neural networks - often with substantial parameter counts. However, these approaches incur significant overhead, as training and deploying large reward models consume substantial computational resources and require large amount of data during both the reward model training phase and the subsequent inference stage [17, 36, 63]. This exclusive reliance on text-based information constrains these models, necessitating large training sets and complex architectures to adequately capture the full spectrum of LLM errors.

Nevertheless, during the inference process, the LLM possesses an inherent ‘inner knowledge’ reflecting its current certainty. Existing research demonstrates that the LLM’s internal states during reasoning contain high levels of information about answer confidence, often captured through *linear* representations [54, 61]. Our preliminary experiment in Section 4.1 also supports this observation by showing that hidden states can encode a *linear* representation for reasoning’s correctness with high accuracy. This property is significant because it suggests that **we can shift our focus on the data source**, that is, we can find the path to efficient reward modeling through developing effective techniques to mine the intrinsic signals already present within the task-performing LLM itself, instead of collecting ever-larger text data or building ever-larger external models.

However, utilizing this property in practice presents a fundamental architectural challenge. Conventional reward models, which are themselves typically fine-tuned LLMs, are engineered to process sequences of discrete text tokens. Their internal mechanisms are entirely optimized for text data, creating an architectural mismatch with the continuous, high-dimensional vectors of hidden states. Simply feeding these latent representations into a text-based model is not a viable path. This necessitates a paradigm shift in reward modeling: the development of a novel architecture specifically designed to mine these intrinsic signals directly from the source.

While prior work has applied probes on hidden states to improve LLM’s reasoning performance, they often focus on the final answer token [3, 7, 54] or on specific answer tokens within each reasoning step [61]. This approach has limitations: relying on a single token’s

Permission to make digital or hard copies of all or part of this work for personal or classroom use is granted without fee provided that copies are not made or distributed for profit or commercial advantage and that copies bear this notice and the full citation on the first page. Copyrights for components of this work owned by others than the author(s) must be honored. Abstracting with credit is permitted. To copy otherwise, or republish, to post on servers or to redistribute to lists, requires prior specific permission and/or a fee. Request permissions from [permissions@acm.org](mailto:permissions@acm.org).

Conference acronym 'XX, Woodstock, NY

© 2018 Copyright held by the owner/author(s). Publication rights licensed to ACM.

ACM ISBN 978-1-4503-XXXX-X/2018/06

<https://doi.org/XXXXXXX.XXXXXXX>

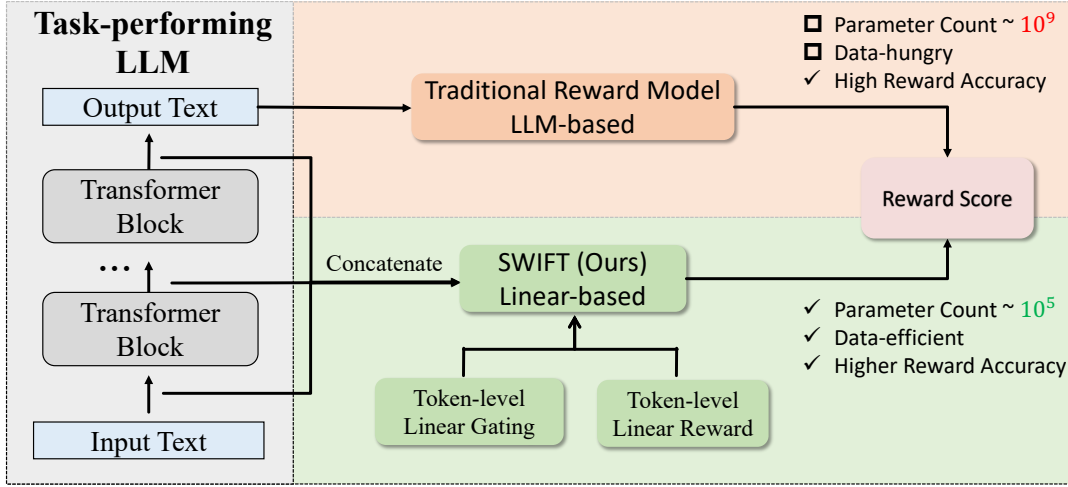


Figure 1: An illustration comparing traditional reward model and SWIFT.

hidden state may not capture the full context of the reasoning process, and defining clear reasoning steps and identifying their corresponding answer tokens can be subjective and challenging. In addition, they do not provide direct reward signals, and their performance gains are limited compared to large-scale reward models.

To solve above challenge, we propose the Simple Weighted Intrinsic Feedback Technique (SWIFT) (illustrated in Figure 1). SWIFT learns a linear gating and a linear reward projection per token. The final reward is computed as a weighted average of these token-level rewards, scaled by the gating values. Our experiments demonstrate that SWIFT **systematically outperforms baseline reward models** while using **fewer than 0.005% their parameters**. Moreover, SWIFT is data-efficient and can be trained using only a few instances. Critically, SWIFT achieves **orders-of-magnitude improvements of efficiency** in average time and FLOPs per sample compared to baselines.

In summary, this work makes three main contributions:

- By changing the data source from text to LLM’s hidden states, we introduce SWIFT, a novel token-level reward-modeling approach. SWIFT outperforms baselines with orders-of-magnitude less parameters and computational cost.
- SWIFT demonstrates exceptional data efficiency and scalability, performing well with limited data, demonstrating performance upgrade with training-time scaling and test-time scaling.
- Experiments also support that SWIFT generalizes to logit-only training for certain closed-source LLMs, and can be combined with conventional reward models to yield further performance improvements.

## 2 Related Work

*Reward Modeling for Language Models’ Reasoning.* The rapid advancement of Large Language Models (LLMs) in complex tasks, such as answering user’s questions [35, 46] and reasoning [56, 64], has highlighted the pivotal role of reward modeling in both training and post-training inference [11, 26]. Current reward models typically

build upon an LLM backbone, with substantial parameter count and requires significant amount of data for training, which introduces high computational costs [17, 36]. Although prior work has proposed various approaches to mitigate such issue [8, 15], achieving a satisfactory balance between efficiency and performance remains a challenge. This work introduces a novel perspective by leveraging internal representations to achieve a significant improvement in efficiency with satisfactory performance.

*Understanding and Leveraging the Internal Representations of Language Models.* The rapid development of LLMs has spurred considerable research into their internal representations [13, 27]. Hidden states of LLMs have been effectively utilized in diverse fields, including safety alignment [5, 66], faithfulness and hallucination detection [7, 19], knowledge editing [32, 58], and knowledge distillation or transfer [12, 53]. By contrast, we effectively leverage the hidden states in intermediate layers of LLMs as a direct signal for reward modeling in reasoning tasks.

## 3 Problem Statement

A common approach to enhance LLM reasoning is best-of-N sampling [47]. Let  $\mathcal{V}$  be the token vocabulary and let  $\mathcal{D}$  be a distribution over problem-answer pairs  $(x, y) \in \mathcal{V}^n \times \mathcal{Y}$ , where  $y$  is the hidden reference solution for question  $x$ . Conditioned on  $x$ , the base LLM  $\pi$  draws  $N$  reasoning paths independently (i.i.d. draws from  $\pi(\cdot | x)$ ), producing  $r_i = (r_{i,1}, \dots, r_{i,m_i}) \in \mathcal{V}^{m_i}$ ,  $i = 1, \dots, N$ , where  $m_i$  is the random length of the  $i$ -th path. We write  $\mathcal{V}^* = \bigcup_{\ell=0}^{\infty} \mathcal{V}^{\ell}$ . Simultaneously,  $\pi$  emits hidden states  $h_i = (h_{i,1}, \dots, h_{i,m_i}) \in (\mathbb{R}^{L \times d})^{m_i}$ , where  $L$  is the number of transformer layers,  $d$  is the per-layer hidden-state dimension, and each  $h_{i,j} \in \mathbb{R}^{L \times d}$  is the stacked hidden state after emitting  $r_{i,j}$ . Define the correctness indicator  $F : \mathcal{V}^* \times \mathcal{Y} \rightarrow \{0, 1\}$ , s.t.  $F(r, y) = 1 \iff r$  yields the reference answer  $y$ . We write  $(\mathbb{R}^{L \times d})^* = \bigcup_{k=0}^{\infty} (\mathbb{R}^{L \times d})^k$ . A parametric reward model  $R_{\theta} : (\mathbb{R}^{L \times d})^* \rightarrow \mathbb{R}$  assigns a scalar score to each  $h_i$  (hence for each  $r_i$ ). Note that neither  $\pi$  nor  $R_{\theta}$  sees  $y$ . At test time we select  $i^* = \arg \max_{1 \leq i \leq N} R_{\theta}(h_i)$  and return  $r_{i^*}$ . Our goal is to choose  $\theta$  to

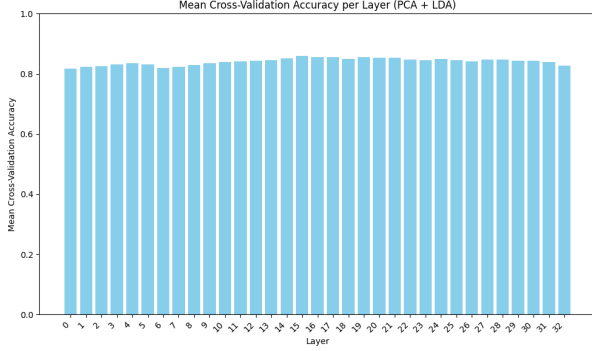


**Figure 2: Cross-validation accuracy of the PCA+LDA pipeline for predicting correctness at each layer of Llama-3.1-8B. The results demonstrate that hidden states contain information about reasoning correctness with linear representation.**

maximize the probability that  $r_{i^*}$  is correct (expectation of  $F(r_{i^*}, y)$ ) under  $D$ :

$$\max_{\theta} \mathbb{E}_{(x,y) \sim D} \mathbb{E}_{(r_1, \dots, r_N) \sim \pi(\cdot | x)} [F(r_{\arg \max_i R_{\theta}(h_i)}, y)]. \quad (1)$$

## 4 Methods

### 4.1 Motivation

We first present a preliminary experiment demonstrating the potential for enhancing reasoning using hidden states. Recent work has shown that LLM hidden states contain information about the correctness probability of a given reasoning path, often exhibiting *linear* representations [54, 61]. To verify this, we designed a simple pipeline to predict the correctness of reasoning steps based on the LLM’s hidden states.

Our pipeline extracts hidden states  $h_t^l$  for each token  $t$  at each layer  $l$  from the Llama-3.1-8B-Instruct model [16] during reasoning on the MATH dataset [21], averages the hidden states across all tokens within each reasoning path to obtain a single vector representation  $\bar{h}^l$  for each layer  $l$ , then reduces  $\bar{h}^l$  for each  $l$  to 50 dimensions using Principal Component Analysis (PCA) [51], and classifies the reasoning as correct or incorrect using Linear Discriminant Analysis (LDA) [4]. The pipeline is linear to verify that the hidden states can encode a *linear* representation for confidence of the answer. For more details, please refer to Appendix C.2.

We performed 5-fold cross-validation on 3000 instances of the MATH dataset. For each layer  $l$ , we trained the pipeline on the training folds and evaluated the classification accuracy on the held-out test fold. Figure 2 presents the average cross-validation accuracy for each layer.

As shown in Figure 2, the accuracy is approximately 80% on each layer, indicating a strong signal for reasoning correctness within the hidden states. This result verifies the aforementioned theory and motivates the development of a novel, lightweight, *linear* reward model that directly leverages this information, as described in the following sections.

### 4.2 Our Approach - SWIFT

Therefore, building upon the observation that LLM internal representations exhibit linear properties, we designed SWIFT (Simple Weighted Intrinsic Feedback Technique) model to be a parameter-efficient, linear model, which learns a token-level reward function directly from the concatenated hidden states.

For each token  $t$  in a reasoning path, we concatenate and flatten the hidden states (after residual connection) from all  $L$  layers:  $h_t = [h_t^1; h_t^2; \dots; h_t^L] \in \mathbb{R}^{Ld}$ , where  $d$  is the dimension of the hidden state. We then apply a linear transformation to obtain a gating value  $g_t$  and a token-level reward  $r_t$ :

$$\begin{pmatrix} \tilde{g}_t \\ r_t \end{pmatrix} = W_{SWIFT} h_t + b_{SWIFT} \quad (2)$$

where  $W_{SWIFT} \in \mathbb{R}^{2 \times Ld}$  is the weight matrix,  $b_{SWIFT} \in \mathbb{R}^2$  is the bias vector,  $\tilde{g}_t$  is the pre-activation gating value, and  $r_t$  is the token-level reward. The gating value is then passed through a sigmoid function [20]:

$$g_t = \sigma(\tilde{g}_t) = \frac{1}{1 + e^{-\tilde{g}_t}} \quad (3)$$

The final reward  $R$  for the entire reasoning path is the weighted average of the token-level rewards, using the gating values as weights:

$$R = \frac{\sum_{t=1}^T (g_t \cdot r_t)}{\max\left(\sum_{t=1}^T g_t, \epsilon\right)} \quad (4)$$

where  $T$  is the number of tokens, and  $\epsilon$  is a small constant (e.g.,  $10^{-8}$ ) for numerical stability. This model only contains  $O(L \times d)$  parameters, which is significantly fewer than those in traditional reward models.

Since different tokens contribute differently to the overall correctness, the gating values allow the model to assign higher weights to more important tokens. In addition, we conduct ablation experiment to show that the gating mechanism can improve performance in Appendix D.2.

We use the binary cross-entropy with logits loss [42] for training. Let  $y \in \{0, 1\}$  denote the correctness label of a reasoning path, where  $y = 1$  indicates a correct path and  $y = 0$  indicates an incorrect path. For a path with hidden state representation  $h$ , the model predicts a scalar logit score  $R(h) \in \mathbb{R}$ . The binary cross-entropy with logits loss is:

$$\mathcal{L} = -\frac{1}{N} \sum_{i=1}^N [y_i \cdot \log(\sigma(R(h_i))) + (1 - y_i) \cdot \log(1 - \sigma(R(h_i)))] \quad (5)$$

where  $\sigma(x) = \frac{1}{1 + e^{-x}}$  is the sigmoid function.

Although binary cross-entropy with logits loss generally yields good results, our experiments detailed in Appendix D.1 demonstrate that DPO [43] and hinge loss [44] can also perform well, sometimes even surpassing cross-entropy. However, given that cross-entropy performs best on average, we adopt it as our primary loss function in the main text. A comparison study among several loss functions is provided in Appendix D.1

## 5 Experiments

### 5.1 Experimental Setup

Our experiments are conducted across mathematical reasoning, code comprehension, commonsense abilities and symbolic reasoning tasks. We evaluate our method on the MATH [21], GSM8K [10], AQuA\_RAT [28], Imbue Code Comprehension [23], HellaSwag [60] and CoinFlip [50] datasets. The models used for generation are Llama-3.2-3B-Instruct [33], Llama-3.1-8B-Instruct [16], and Ministral-8B-Instruct [34]. The generation temperature is 1.0 with  $\text{top}_p$  to be 0.9. We use 6000 instances (each with 8 reasoning paths) for training and 500 instances for evaluation. When training SWIFT, we use early stopping [57] based on validation set performance to mitigate overfitting. For more details on the generation process, training and evaluation, please refer to Appendix C.3, C.4 and C.5.

We compare our method against six recent open-source reward models: EururRM-7B [59], Skywork-Reward-Llama-3.1-8B-v0.2 [29], Starling-7B [65], UltraRM-13B [11], RLHFlow-8B-Deepseek [55], Math-Shepherd-7B [49]. These baselines are very parameter heavy and trained on extensive datasets, while achieving leading performance among open-source reward models. **These six baseline reward models have all been explicitly trained on data related to reasoning and code domains. Their enhanced performance in these specific areas is well-documented and validated in their respective original publications.** It is particularly noteworthy that the development of Eurur-7B, Ultra-13B, RLHFlow-8B-Deepseek, and Math-Shepherd-7B involved training and evaluation on the MATH and GSM8K datasets. This corresponds directly with the datasets used in our work, confirming the relevance of these models as strong baselines.

For links and brief descriptions of baselines, please refer to Appendix A. For parameter count and training data size of baselines compared against SWIFT, see Table 3 for details.

To provide a more comprehensive comparison, we also evaluated a fine-tuned version of EururRM-7B, detailed in Appendix C.6, specifically fine-tuned on the relevant datasets and model-generated solutions used in our experiments, while using the same loss function as in the original publication to ensure consistency. This is despite EururRM-7B already being pre-trained on MATH and GSM8K, which gives it a potential advantage.

### 5.2 Accuracy

Table 1 reports the Best-of-N performance on mathematics domain of each reward model on the MATH, GSM8K, and AQuA\_RAT datasets, and Table 2 reports their performance on other general domains, including code comprehension (Imbue Code Comprehension dataset), commonsense (HellaSwag dataset) and symbolic reasoning (CoinFlip dataset). Our SWIFT model **outperforms all baseline reward models** across most BoN settings, demonstrating the effectiveness of the proposed linear architecture and hinge-loss training objective. A notable observation is that while many baseline reward models exhibit strong performance on specific subsets of the data, SWIFT demonstrates consistent and robust performance across the entire dataset. While the fine-tuned EururRM-7B delivers respectable results, it still lags behind SWIFT in accuracy and incurs

substantially higher computational costs during both training and inference. In contrast, SWIFT not only achieves the best performance but does so with a parameter footprint less than 0.005% that of the baselines and is trained on only 6,000 samples per dataset (see Section 5.3 for detailed comparison). This underscores the exceptional efficiency of our approach.

It is noteworthy that the results presented here were achieved **without extensive hyperparameter tuning**. Further performance gains could likely be realized through more refined optimization strategies. For example, exploring alternative loss functions, as demonstrated in Appendix Table 6, increasing the training dataset size based on the scalability analysis in Section 5.4, or training SWIFT on a subset of layers as explored in Section 5.5 (Table 4), could yield further improvements. This suggests that SWIFT has significant potential for further optimization and improvement.

### 5.3 Efficiency Analysis

We demonstrate SWIFT’s significant parameter efficiency and data efficiency in Table 3. Moreover, we investigate the computational efficiency of SWIFT by comparing the average time and FLOPs required to assign a reward to each sample. Figure 3 presents a comparative analysis of SWIFT and baseline reward models across various datasets and task-performing models. The results reveal that SWIFT achieves orders-of-magnitude improvements in both time and FLOPs compared to the baselines. It is noteworthy that as shown in Section 5.4, even a much smaller training dataset leads to satisfactory performance. This substantial reduction in computational cost, combined with its parameter efficiency and data efficiency, makes SWIFT a highly practical solution for reward modeling in both resource-constrained environments and large-scale applications.

**Table 3: Comparison of Reward Model Parameters and Training Data Size (number of questions  $\times$  number of answers). Our method is remarkably efficient in terms of parameters and data.**

Reward Model	Parameters	Training data size
Eurus-7B	$7.1 \times 10^9$	$5.8 \times 10^5 \times 2$
Skywork-Llama3.1-8B	$7.5 \times 10^9$	$8.0 \times 10^4 \times 2$
Starling-7B	$6.7 \times 10^9$	$1.8 \times 10^5 \times 7$
Ultra-13B	$1.3 \times 10^{10}$	$7.5 \times 10^5 \times 2$
RLHFlow-8B-Deepseek	$8.0 \times 10^9$	$2.5 \times 10^5 \times 1$
Math-Shepherd-7B	$7.2 \times 10^9$	$4.5 \times 10^5 \times 1$
SWIFT (on Llama-3.2-3B)	$1.8 \times 10^5$	$6.0 \times 10^3 \times 8$
SWIFT (on Llama-3.1-8B)	$2.7 \times 10^5$	$6.0 \times 10^3 \times 8$
SWIFT (on Ministral-8B)	$3.0 \times 10^5$	$6.0 \times 10^3 \times 8$

### 5.4 Scalability with Training Set Size and Reasoning Paths

Scaling large language models (LLMs) can be achieved through various strategies, broadly categorized as training-time scaling and

**Table 1: Different methods’ best-of-N sampling performance on mathematics domain, including MATH, GSM8K, and AQuA\_RAT datasets. Results represent accuracy (percentages omitted). Our method outperforms baselines. Bold: best performance; Underline: second-best performance; @k: indicates the number of reasoning paths used in best-of-N sampling.**

MATH Dataset										
Reward Model	Llama-3.2-3B BoN@1: 39.0			Llama-3.1-8B BoN@1: 47.2			Ministral-8B BoN@1: 51.0			Avg.
	@4	@16	@64	@4	@16	@64	@4	@16	@64	
Eurus-7B	42.6	48.2	46.8	50.8	52.0	52.2	54.6	56.8	55.0	51.0
Skywork-Llama3.1-8B	43.8	<u>48.4</u>	<u>48.8</u>	52.2	52.4	<u>53.4</u>	<u>56.8</u>	<u>59.0</u>	<u>61.6</u>	<u>52.9</u>
Starling-7B	39.6	41.2	39.8	50.4	49.0	49.0	53.8	50.2	47.0	46.7
Ultra-13B	<u>44.6</u>	47.4	44.4	<u>53.0</u>	50.6	50.4	53.6	53.0	54.0	50.1
RLHFlow-8B-Deepseek	43.2	46.4	47.6	51.2	49.6	49.8	56.2	58.4	57.8	51.1
Math-Shepherd-7B	43.8	42.6	43.6	48.8	50.8	49.0	55.8	58.8	54.8	49.8
Fine-tuned Eurus-7B	42.2	47.0	46.6	51.8	<u>53.0</u>	50.2	54.8	57.2	57.2	51.1
SWIFT (ours)	<b>49.8</b>	<b>54.6</b>	<b>53.6</b>	<b>55.4</b>	<b>59.4</b>	<b>62.6</b>	<b>57.8</b>	<b>61.6</b>	<b>62.8</b>	<b>57.5</b>
GSM8K Dataset										
Reward Model	Llama-3.2-3B BoN@1: 53.0			Llama-3.1-8B BoN@1: 80.4			Ministral-8B BoN@1: 79.6			Avg.
	@4	@16	@64	@4	@16	@64	@4	@16	@64	
Eurus-7B	69.8	76.2	82.4	87.0	89.0	90.4	87.0	90.8	90.4	84.8
Skywork-Llama3.1-8B	77.2	81.8	85.2	89.6	89.4	89.2	83.0	85.8	87.4	85.4
Starling-7B	62.4	65.6	71.4	83.0	87.2	85.4	78.4	81.2	80.0	77.2
Ultra-13B	72.6	78.6	82.4	88.0	88.6	86.8	82.6	84.6	82.0	82.9
RLHFlow-8B-Deepseek	52.4	53.8	60.0	80.4	77.0	80.0	<u>88.4</u>	91.2	<b>93.4</b>	75.2
Math-Shepherd-7B	54.8	49.8	43.4	80.6	75.4	73.0	84.8	86.8	86.8	70.6
Fine-tuned Eurus-7B	<u>79.2</u>	<u>84.4</u>	<u>86.8</u>	<u>90.0</u>	<b>91.2</b>	<b>91.0</b>	88.2	<u>91.8</u>	92.8	<u>88.4</u>
SWIFT (ours)	<b>80.0</b>	<b>86.4</b>	<b>87.6</b>	<b>90.6</b>	<u>89.6</u>	<u>90.6</u>	<b>89.8</b>	<b>93.2</b>	<b>93.4</b>	<b>89.0</b>
AQuA_RAT Dataset										
Reward Model	Llama-3.2-3B BoN@1: 42.0			Llama-3.1-8B BoN@1: 53.6			Ministral-8B BoN@1: 56.6			Avg.
	@4	@16	@64	@4	@16	@64	@4	@16	@64	
Eurus-7B	44.6	42.8	44.6	58.6	60.6	56.8	48.4	34.6	27.2	46.5
Skywork-Llama3.1-8B	<u>60.4</u>	<u>68.0</u>	<u>69.4</u>	<u>69.0</u>	<b>77.0</b>	<b>79.2</b>	65.6	71.2	<u>72.0</u>	<u>70.2</u>
Starling-7B	51.4	55.0	56.6	<u>64.2</u>	70.8	69.8	56.4	48.6	42.8	57.3
Ultra-13B	58.4	61.6	64.8	67.4	<u>72.8</u>	71.8	58.4	51.4	48.0	61.6
RLHFlow-8B-Deepseek	53.8	54.0	48.8	63.6	65.0	61.4	64.6	63.8	62.6	59.7
Math-Shepherd-7B	52.2	53.4	53.0	64.0	67.8	66.2	63.6	60.4	60.2	60.1
Fine-tuned Eurus-7B	57.4	66.6	62.0	68.8	<u>72.8</u>	69.8	<u>71.2</u>	<u>71.8</u>	71.0	67.9
SWIFT (ours)	<b>61.0</b>	<b>70.4</b>	<b>70.8</b>	<b>69.6</b>	<b>77.0</b>	<u>77.0</u>	<b>75.2</b>	<b>75.8</b>	<b>78.0</b>	<b>72.8</b>

test-time scaling [24, 47]. In this section, we investigate the scalability of SWIFT with respect to both training set size and the number of reasoning paths used during inference.

From Figure 4, our results demonstrate that SWIFT’s accuracy consistently improves with both the number of training samples and the size of the reasoning paths set. Specifically, under different

BoN@k settings, we find that SWIFT’s accuracy increases monotonically with training set size. Likewise, for any given training set size, SWIFT’s accuracy also improves as the number of reasoning paths used in the BoN sampling process increases.

It is interesting to note that, as illustrated in Figure 4, the performance of SWIFT with training-time scaling has not appeared to saturate even when there are 6000 training samples, which is the one

**Table 2: Different methods’ best-of-N sampling performance on general domain, including Imbue Code Comprehension, HellaSwag and CoinFlip datasets. Results represent accuracy (percentages omitted). Our method outperforms baselines. Bold: best performance; Underline: second-best performance; @k: indicates the number of reasoning paths used in best-of-N sampling.**

Imbue Code Comprehension Dataset										
Reward Model	Llama-3.2-3B BoN@1: 17.2			Llama-3.1-8B BoN@1: 47.6			Ministral-8B BoN@1: 54.4			Avg.
	@4	@16	@64	@4	@16	@64	@4	@16	@64	
Eurus-7B	26.0	28.0	30.2	60.0	62.2	66.2	59.0	61.6	64.0	50.8
Skywork-Llama3.1-8B	32.6	47.4	56.0	<u>67.0</u>	70.8	75.2	66.6	71.4	74.8	62.4
Starling-7B	18.8	21.0	21.0	<u>57.6</u>	62.6	64.2	58.6	60.4	62.6	47.4
Ultra-13B	28.0	34.8	38.8	61.8	66.6	68.6	60.6	64.4	65.2	54.3
RLHFlow-8B-Deepseek	29.2	37.0	44.4	66.4	<u>71.4</u>	72.0	<u>68.4</u>	<u>74.0</u>	<u>75.2</u>	59.8
Math-Shepherd-7B	22.6	25.4	25.4	60.6	60.0	55.8	63.0	65.4	61.4	48.8
Fine-tuned Eurus-7B	<u>35.6</u>	<u>54.4</u>	<u>60.4</u>	<u>67.0</u>	69.4	<u>76.0</u>	67.8	71.0	71.8	<u>63.7</u>
SWIFT (ours)	<b>36.8</b>	<b>57.6</b>	<b>65.6</b>	<b>74.0</b>	<b>84.0</b>	<b>85.0</b>	<b>74.6</b>	<b>82.4</b>	<b>85.4</b>	<b>71.7</b>
HellaSwag Dataset										
Reward Model	Llama-3.2-3B BoN@1: 55.2			Llama-3.1-8B BoN@1: 61.2			Ministral-8B BoN@1: 68.2			Avg.
	@4	@16	@64	@4	@16	@64	@4	@16	@64	
Eurus-7B	67.4	71.6	72.0	72.6	73.6	74.0	77.8	77.4	78.0	73.8
Skywork-Llama3.1-8B	63.0	64.0	67.0	70.6	71.6	71.8	73.0	74.0	76.4	70.2
Starling-7B	53.6	56.2	59.0	64.8	65.8	63.6	66.0	65.0	63.6	62.0
Ultra-13B	60.8	64.0	64.2	69.6	69.4	68.2	67.8	67.8	70.6	66.9
RLHFlow-8B-Deepseek	65.2	68.4	69.2	68.2	70.8	71.0	75.2	78.2	79.8	71.8
Math-Shepherd-7B	59.8	61.0	62.2	66.0	65.2	63.8	70.2	69.8	73.0	65.7
Fine-tuned Eurus-7B	<u>70.4</u>	<b>76.2</b>	<b>77.4</b>	<u>75.2</u>	<u>79.4</u>	<u>78.6</u>	<u>80.4</u>	<u>81.4</u>	<u>81.6</u>	<u>77.8</u>
SWIFT (ours)	<b>71.0</b>	<u>75.8</u>	<u>77.4</u>	<b>78.0</b>	<b>82.4</b>	<b>83.2</b>	<b>83.4</b>	<b>88.0</b>	<b>88.2</b>	<b>80.8</b>
CoinFlip Dataset										
Reward Model	Llama-3.2-3B BoN@1: 56.2			Llama-3.1-8B BoN@1: 62.6			Ministral-8B BoN@1: 20.0			Avg.
	@4	@16	@64	@4	@16	@64	@4	@16	@64	
Eurus-7B	65.6	64.2	64.6	83.6	85.6	91.8	45.8	69.8	77.4	72.0
Skywork-Llama3.1-8B	72.6	81.0	88.0	88.0	94.4	97.4	25.2	28.2	26.0	66.8
Starling-7B	66.6	73.0	76.2	79.0	84.2	87.2	22.0	19.6	21.0	58.8
Ultra-13B	61.6	62.0	59.4	82.0	85.6	84.0	14.0	11.4	11.4	52.4
RLHFlow-8B-Deepseek	64.0	65.6	75.6	83.4	96.4	99.4	34.6	49.4	72.8	71.2
Math-Shepherd-7B	55.8	46.4	35.4	62.4	40.4	15.2	20.0	19.0	15.4	34.4
Fine-tuned Eurus-7B	<u>91.2</u>	<u>99.4</u>	<u>99.8</u>	<u>95.2</u>	<b>99.8</b>	<b>100.0</b>	<b>57.8</b>	<u>95.8</u>	<b>99.8</b>	<u>93.2</u>
SWIFT (ours)	<b>91.6</b>	<b>99.8</b>	<b>100.0</b>	<b>95.4</b>	<u>99.6</u>	<b>100.0</b>	<b>57.8</b>	<b>96.2</b>	<u>99.6</u>	<b>93.3</b>

used in the experiments of Section 5.2. This suggests that further increasing the training set size may lead to even greater performance improvements, highlighting the scalability of SWIFT. This indicates that SWIFT is a compelling way to scale reward modeling and hence is a practical solution for real-world applications.

## 5.5 Maintaining Performance with Selective Layer Utilization for Higher Efficiency

While SWIFT leverages hidden states from all layers of the LLM, we investigated the potential for further parameter reduction by selectively utilizing hidden states from a subset of layers. Specifically,

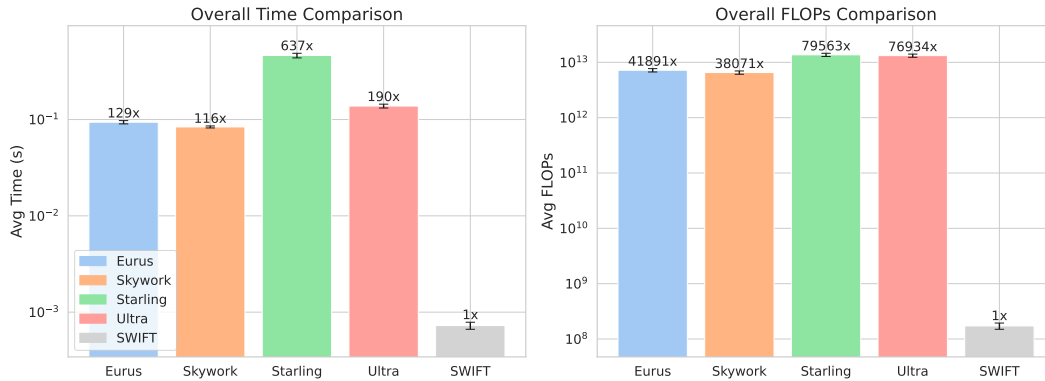


**Figure 3: Comparison of average time and FLOPs per sample for SWIFT and baselines, averaged across different datasets and task-performing models with 1-sigma error bars using standard error of the mean. The y-axis is plotted in log-scale. The results show that SWIFT achieves orders-of-magnitude higher efficiency than the baselines. See Appendix Figure 6 for full details.**

**Table 4: SWIFT’s high Best-of-N sampling performance is maintained even when trained only on layers 16, 24, 28, and 32 for Llama-3.1-8B, leading to a substantial reduction in parameters and improved efficiency.**

Method	MATH BoN@1: 47.2			GSM8K BoN@1: 80.4			AQuA_RAT BoN@1: 53.6			Avg.
	@4	@16	@64	@4	@16	@64	@4	@16	@64	
SWIFT on partial layers	55.8	59.0	60.0	89.4	90.8	92.0	69.6	76.8	77.4	74.5
SWIFT on all layers	55.4	59.4	62.6	90.6	89.6	90.6	69.6	77.0	77.0	74.6

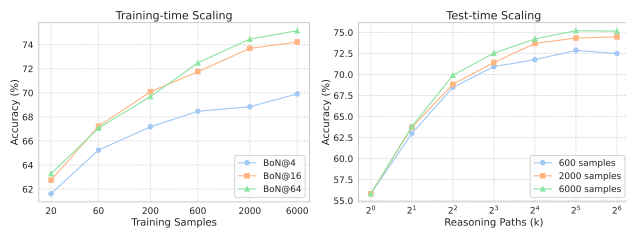


**Figure 4: SWIFT has positive scaling with increased number of training samples and with the number of reasoning paths for inference. The result is averaged across datasets and task-performing models. See Appendix Figure 7 for full results.**

for the Llama-3.1-8B model, which comprises 32 layers (plus an embedding layer), we explored training SWIFT using only the hidden states from layers 16, 24, 28, and 32, following the setting in Azaria and Mitchell [3]. This configuration reduces the parameter count to approximately 4/33 of the full-layer SWIFT model. The results, presented in Table 4, demonstrate that performance remains comparable to the full-layer SWIFT, with certain settings even showing improved accuracy. Notably, on the GSM8K dataset, the BoN@16 and BoN@64 accuracies surpass those of the full-layer SWIFT. As shown in Table 1, the performance of the layer-selected SWIFT also

consistently exceeds that of baselines with significantly larger parameter counts, further underscoring the efficiency and effectiveness of our approach.

## 5.6 Logit-Based Training for Closed-Source LLMs

While SWIFT offers significant advantages in terms of efficiency and performance, making it well-suited for deployment by large model providers and end-users, a limitation arises when dealing with closed-source LLMs where hidden states are inaccessible. To overcome this constraint, we leverage the fact that some closed-source models still provide access to their logits, such as GPT-3.5-turbo [37] and GPT-4 [1], as illustrated in Finlayson et al. [14] and OpenAI [38]. We train SWIFT directly on these logits, resulting in a model with a parameter count that is orders of magnitude smaller than traditional reward models - and even smaller than SWIFT trained on all layers. This allows for effortless deployment on personal devices such as smartphones and personal computers. As demonstrated in Table 5 and Appendix Table 9, the resulting logit-based SWIFT retains strong performance. Furthermore, as shown in Table 1, its performance even surpasses that of many baselines. These results highlight the versatility and adaptability of SWIFT, making it a viable solution even when access to hidden states is restricted.

**Table 5: Training SWIFT solely on logits can also yield high performance and can outperform many baselines with orders-of-magnitude higher efficiency. For results on GSM8K and AQuA\_RAT dataset, please refer to Appendix Table 9.**

MATH Dataset										
Method	Llama-3.2-3B BoN@1: 39.0			Llama-3.1-8B BoN@1: 47.2			Ministral-8B BoN@1: 51.0			Avg.
	@4	@16	@64	@4	@16	@64	@4	@16	@64	
SWIFT on logits	44.6	49.6	50.6	54.2	54.4	55.8	53.4	55.6	57.4	52.8

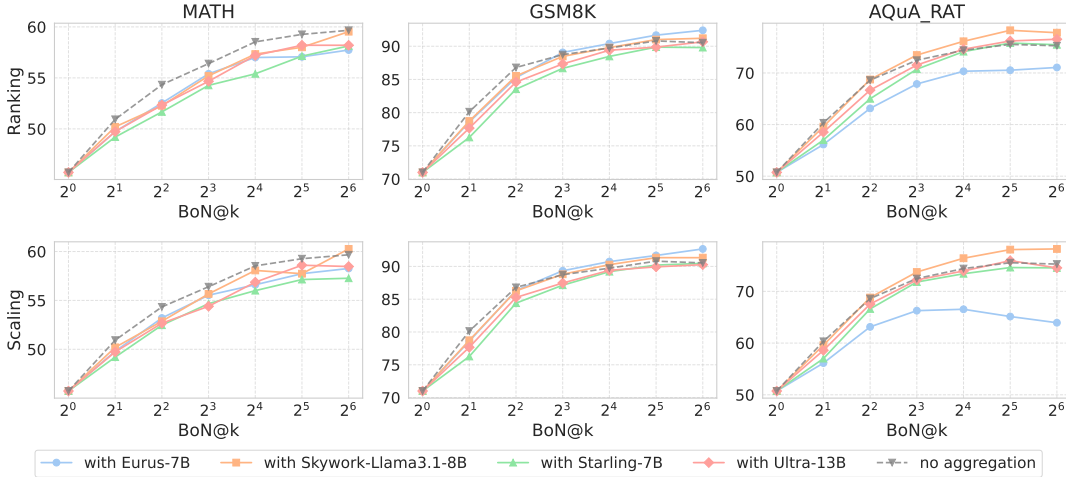


**Figure 5: Average performance of combined SWIFT and external reward models across different datasets and task-performing models, for both rank selection and scaled averaging. See Appendix Figure 8 for full details.**

### 5.7 Combining SWIFT with External Reward Models

SWIFT offers a highly parameter-efficient approach to reward modeling, enabling its seamless integration with existing external reward models. Given SWIFT’s minimal parameter footprint (less than 0.005% of baseline models), the additional computational overhead introduced by incorporating SWIFT is negligible compared to relying solely on the external reward model. We explore two straightforward methods for combining SWIFT with external rewards: rank selection and scaled averaging. In rank selection, we choose the sample with the lowest (i.e. best) rank as determined by either SWIFT or the external reward model. In scaled averaging, we average the rewards from both models after normalizing them to the [0, 1] range. Detailed descriptions of these methods are provided in Appendix B.

We empirically evaluated the effectiveness of these combination strategies by integrating SWIFT with various traditional reward models across different datasets and task-performing models, assessing performance using best-of-N sampling. Figure 5 presents the average results across different datasets for both ranking and scaling methods, applied to various task-performing models. Detailed results for each dataset and task-performing model can be found in Appendix Figure 8. Our findings indicate that combining SWIFT with external reward models can lead to further improvements in accuracy, particularly on the GSM8K and AQuA-RAT datasets. The

MATH dataset did not exhibit significant performance gains, potentially because SWIFT already significantly outperforms the external reward models on this benchmark. This performance boost is likely due to SWIFT and external reward models capturing different types of errors, resulting in improved overall accuracy-particularly with a higher number of best-of-N reasoning paths. This combination strategy offers a pathway to achieve further performance gains without incurring significant computational overhead.

### 5.8 Analysis on SWIFT

To investigate the mechanism of SWIFT, we present illustrative examples of its scoring of reasoning paths in Appendix E. The examples with the highest and lowest gating × reward values are highlighted, along with their corresponding numerical scores. Notably, SWIFT assigns relatively high or low gating × reward values to specific numerical and mathematical symbols, as well as particular tokens such as “answer”, “boxed” and the special token ‘<|eot\_id|>’. This behavior suggests that SWIFT possesses the ability to identify and weigh key components within the reasoning process.

## 6 Conclusion

In this paper, we presented SWIFT (Simple Weighted Intrinsic Feedback Technique), a novel reward modeling approach for large language models (LLMs) that leverages the rich information in the LLM’s internal hidden states with significant efficiency and efficacy.

Admittedly, this work has some limitations. SWIFT’s reliance on access to the LLM’s hidden states or logits makes it potentially less applicable to commercial LLMs that do not expose these information to users. However, the efficiency and ease of deployment with SWIFT ensure that it is well-suited to LLM providers themselves. In addition, SWIFT should be trained individually for each LLM. However, given the small model size and limited data required, the associated computational overhead is negligible, especially when compared to the cost of training the task-performing LLM itself.

## Acknowledgments

We gratefully acknowledge Mrs. Jiahe Jin from Zhiyuan College, Shanghai Jiao Tong University, for her invaluable assistance in creating the initial version of our illustrations. We also thank Mr. Zhihui Xie from The University of Hong Kong for offering precious suggestions.

## References

- [1] Josh Achiam, Steven Adler, Sandhini Agarwal, Lama Ahmad, Ilge Akkaya, Florencia Leoni Aleman, Diogo Almeida, Janko Altschmidt, Sam Altman, Shyamal Anadkat, et al. 2023. Gpt-4 technical report. *arXiv preprint arXiv:2303.08774* (2023).
- [2] Reza Yazdani Aminabadi, Samyam Rajbhandari, Ammar Ahmad Awan, Cheng Li, Du Li, Elton Zheng, Olatunji Ruwase, Shaden Smith, Minjia Zhang, Jeff Rasley, et al. 2022. DeepSpeed-Inference: enabling efficient inference of transformer models at unprecedented scale. In *SC22: International Conference for High Performance Computing, Networking, Storage and Analysis*. IEEE, 1–15.
- [3] Amos Azaria and Tom Mitchell. 2023. The Internal State of an LLM Knows When It’s Lying. In *Findings of the Association for Computational Linguistics: EMNLP 2023*, Houda Bouamor, Juan Pino, and Kalika Bali (Eds.). Association for Computational Linguistics, Singapore, 967–976. <https://doi.org/10.18653/v1/2023.findings-emnlp.68>
- [4] Suresh Balakrishnama and Aravind Ganapathiraju. 1998. Linear discriminant analysis—a brief tutorial. *Institute for Signal and information Processing* 18, 1998 (1998), 1–8.
- [5] Fazl Barez, Tingchen Fu, Ameya Prabhu, Stephen Casper, Amartya Sanyal, Adel Bibi, Aidan O’Gara, Robert Kirk, Ben Bucknall, Tim Fist, et al. 2025. Open problems in machine unlearning for ai safety. *arXiv preprint arXiv:2501.04952* (2025).
- [6] Neil Burgess, Jelena Milanovic, Nigel Stephens, Konstantinos Monachopoulos, and David Mansell. 2019. Bfloat16 processing for neural networks. In *2019 IEEE 26th Symposium on Computer Arithmetic (ARITH)*. IEEE, 88–91.
- [7] Collin Burns, Haotian Ye, Dan Klein, and Jacob Steinhardt. 2023. Discovering Latent Knowledge in Language Models Without Supervision. In *The Eleventh International Conference on Learning Representations*. <https://openreview.net/forum?id=ETKGubY0hcs>
- [8] Alex J Chan, Hao Sun, Samuel Holt, and Mihaela Van Der Schaar. 2024. Dense reward for free in reinforcement learning from human feedback. *arXiv preprint arXiv:2402.00782* (2024).
- [9] Huayu Chen, Guande He, Lifan Yuan, Ganqu Cui, Hang Su, and Jun Zhu. 2024. Noise Contrastive Alignment of Language Models with Explicit Rewards. In *The Thirty-eighth Annual Conference on Neural Information Processing Systems*. <https://openreview.net/forum?id=KwRLDkyVOI>
- [10] Karl Cobbe, Vineet Kosaraju, Mohammad Bavarian, Mark Chen, Heewoo Jun, Lukasz Kaiser, Matthias Plappert, Jerry Tworek, Jacob Hilton, Reiichiro Nakano, Christopher Hesse, and John Schulman. 2021. Training Verifiers to Solve Math Word Problems. *arXiv preprint arXiv:2110.14168* (2021).
- [11] Ganqu Cui, Lifan Yuan, Ning Ding, Guanming Yao, Bingxiang He, Wei Zhu, Yuan Ni, Guotong Xie, Ruobing Xie, Yankai Lin, Zhiyuan Liu, and Maosong Sun. 2024. ULTRAFEEBACK: Boosting Language Models with Scaled AI Feedback. In *Forty-first International Conference on Machine Learning*. <https://openreview.net/forum?id=BOorDpKHij>
- [12] Sayantan Dasgupta and Trevor Cohn. 2025. Improving Language Model Distillation through Hidden State Matching. In *The Thirteenth International Conference on Learning Representations*. <https://openreview.net/forum?id=IcVSKhVpKu>
- [13] Javier Ferrando, Gabriele Sarti, Arianna Bisazza, and Marta R Costa-Jussà. 2024. A primer on the inner workings of transformer-based language models. *arXiv preprint arXiv:2405.00208* (2024).
- [14] Matthew Finlayson, Xiang Ren, and Swabha Swayamdipta. 2024. Logits of API-Protected LLMs Leak Proprietary Information. In *First Conference on Language Modeling*. <https://openreview.net/forum?id=oRcYFm8vyB>
- [15] Adam Fisch, Jacob Eisenstein, Vicky Zayats, Alekh Agarwal, Ahmad Beirami, Chirag Nagpal, Pete Shaw, and Jonathan Berant. 2024. Robust preference optimization through reward model distillation. *arXiv preprint arXiv:2405.19316* (2024).
- [16] Aaron Grattafiori, Abhimanyu Dubey, Abhinav Jauhri, Abhinav Pandey, Abhishek Kadian, Ahmad Al-Dahle, Aiesha Letman, Akhil Mathur, Alan Schelten, Alex Vaughan, et al. 2024. The llama 3 herd of models. *arXiv preprint arXiv:2407.21783* (2024).
- [17] Daya Guo, Dejian Yang, Haowei Zhang, Junxiao Song, Ruoyu Zhang, Runxin Xu, Qihao Zhu, Shirong Ma, Peiyi Wang, Xiao Bi, et al. 2025. Deepseek-r1: Incentivizing reasoning capability in llms via reinforcement learning. *arXiv preprint arXiv:2501.12948* (2025).
- [18] Yiju Guo, Ganqu Cui, Lifan Yuan, Ning Ding, Zexu Sun, Bowen Sun, Huimin Chen, Ruobing Xie, Jie Zhou, Yankai Lin, Zhiyuan Liu, and Maosong Sun. 2024. Controllable Preference Optimization: Toward Controllable Multi-Objective Alignment. In *Proceedings of the 2024 Conference on Empirical Methods in Natural Language Processing*, Yaser Al-Ozaian, Mohit Bansal, and Yun-Nung Chen (Eds.). Association for Computational Linguistics, Miami, Florida, USA, 1437–1454. <https://doi.org/10.18653/v1/2024.emnlp-main.85>
- [19] Avelina Asada Hadji-Kyriacou and Ognjen Arandjelovic. 2024. Would I Lie To You? Inference Time Alignment of Language Models using Direct Preference Heads. In *The Thirty-eighth Annual Conference on Neural Information Processing Systems*. <https://openreview.net/forum?id=NKGulthW80>
- [20] Jun Han and Claudio Moraga. 1995. The influence of the sigmoid function parameters on the speed of backpropagation learning. In *International workshop on artificial neural networks*. Springer, 195–201.
- [21] Dan Hendrycks, Collin Burns, Saurav Kadavath, Akul Arora, Steven Basart, Eric Tang, Dawn Song, and Jacob Steinhardt. 2021. Measuring Mathematical Problem Solving With the MATH Dataset. In *Thirty-fifth Conference on Neural Information Processing Systems Datasets and Benchmarks Track (Round 2)*. <https://openreview.net/forum?id=7Bywt2mQsCe>
- [22] Edward J Hu, Yelong Shen, Phillip Wallis, Zeyuan Allen-Zhu, Yuanzhi Li, Shean Wang, Lu Wang, Weizhu Chen, et al. 2022. Lora: Low-rank adaptation of large language models. *ICLR* 1, 2 (2022), 3.
- [23] Imbue Team. 2024. Sanitized open-source datasets for natural language and code understanding: how we evaluated our 70B model. <https://imbue.com/research/70b-evals/>.
- [24] Jared Kaplan, Sam McCandlish, Tom Henighan, Tom B Brown, Benjamin Chess, Rewon Child, Scott Gray, Alec Radford, Jeffrey Wu, and Dario Amodei. 2020. Scaling laws for neural language models. *arXiv preprint arXiv:2001.08361* (2020).
- [25] Woosuk Kwon, Zhuohan Li, Siyuan Zhuang, Ying Sheng, Lianmin Zheng, Cody Hao Yu, Joseph E. Gonzalez, Hao Zhang, and Ion Stoica. 2023. Efficient Memory Management for Large Language Model Serving with PagedAttention. In *Proceedings of the ACM SIGOPS 29th Symposium on Operating Systems Principles*.
- [26] Nathan Lambert, Valentina Pyatkin, Jacob Morrison, Lester James Validad Miranda, Bill Yuchen Lin, Khyathi Chandu, Nouha Dziri, Sachin Kumar, Tom Zick, Yejin Choi, Noah A. Smith, and Hannaneh Hajishirzi. 2025. RewardBench: Evaluating Reward Models for Language Modeling. In *Findings of the Association for Computational Linguistics: NAACL 2025*, Luis Chiruzzo, Alan Ritter, and Lu Wang (Eds.). Association for Computational Linguistics, Albuquerque, New Mexico, 1755–1797. <https://aclanthology.org/2025.findings-naacl.96/>
- [27] Kenneth Li, Aspen K Hopkins, David Bau, Fernanda Viégas, Hanspeter Pfister, and Martin Wattenberg. 2023. Emergent world representations: Exploring a sequence model trained on a synthetic task. *ICLR* (2023).
- [28] Wang Ling, Dani Yogatama, Chris Dyer, and Phil Blunsom. 2017. Program Induction by Rationale Generation: Learning to Solve and Explain Algebraic Word Problems. In *Proceedings of the 55th Annual Meeting of the Association for Computational Linguistics (Volume 1: Long Papers)*, Regina Barzilay and Min-Yen Kan (Eds.). Association for Computational Linguistics, Vancouver, Canada, 158–167. <https://doi.org/10.18653/v1/P17-1015>
- [29] Chris Yuhao Liu, Liang Zeng, Jiakai Liu, Rui Yan, Jujie He, Chaojie Wang, Shuicheng Yan, Yang Liu, and Yahui Zhou. 2024. Skywork-reward: Bag of tricks for reward modeling in llms. *arXiv preprint arXiv:2410.18451* (2024).
- [30] Xiao Liu, Hanyu Lai, Hao Yu, Yifan Xu, Aohan Zeng, Zhengxiao Du, Peng Zhang, Yuxiao Dong, and Jie Tang. 2023. WebGLM: towards an efficient web-enhanced question answering system with human preferences. In *Proceedings of the 29th ACM SIGKDD conference on knowledge discovery and data mining*. 4549–4560.

- [31] Ilya Loshchilov and Frank Hutter. 2019. Decoupled Weight Decay Regularization. In *International Conference on Learning Representations*. <https://openreview.net/forum?id=Bkg6RiCqY7>
- [32] Kevin Meng, David Bau, Alex Andonian, and Yonatan Belinkov. 2022. Locating and editing factual associations in gpt. *Advances in neural information processing systems* 35 (2022), 17359–17372.
- [33] Meta. 2024. Llama 3.2: Revolutionizing edge AI and vision with open, customizable models. <https://ai.meta.com/blog/llama-3-2-connect-2024-vision-edge-mobile-devices/>.
- [34] Mistral AI. 2024. Introducing the world’s best edge models. <https://mistral.ai/news/ministraux>.
- [35] Fengran Mo, Jian-Yun Nie, Kaiyu Huang, Kelong Mao, Yutao Zhu, Peng Li, and Yang Liu. 2023. Learning to relate to previous turns in conversational search. In *Proceedings of the 29th ACM SIGKDD Conference on Knowledge Discovery and Data Mining*. 1722–1732.
- [36] Hyuk Namgoong, Jeosu Jung, Sangkeun Jung, and YoonHyung Roh. 2024. Exploring Domain Robust Lightweight Reward Models based on Router Mechanism. In *Findings of the Association for Computational Linguistics: ACL 2024*, Lun-Wei Ku, Andre Martins, and Vivek Srikumar (Eds.). Association for Computational Linguistics, Bangkok, Thailand, 8644–8652. <https://doi.org/10.18653/v1/2024.findings-acl.511>
- [37] OpenAI. 2023. GPT-3.5 Turbo. <https://platform.openai.com/docs/models/gpt-3.5-turbo>.
- [38] OpenAI. 2023. Using logprobs. [https://cookbook.openai.com/examples/using\\_logprobs](https://cookbook.openai.com/examples/using_logprobs).
- [39] Long Ouyang, Jeffrey Wu, Xu Jiang, Diogo Almeida, Carroll Wainwright, Pamela Mishkin, Chong Zhang, Sandhini Agarwal, Katarina Slama, Alex Gray, John Schulman, Jacob Hilton, Fraser Kelton, Luke Miller, Maddie Simens, Amanda Askell, Peter Welinder, Paul Christiano, Jan Leike, and Ryan Lowe. 2022. Training language models to follow instructions with human feedback. In *Advances in Neural Information Processing Systems*, Alice H. Oh, Alekh Agarwal, Danielle Belgrave, and Kyunghyun Cho (Eds.). <https://openreview.net/forum?id=TG8KACxEOE>
- [40] Adam Paszke, Sam Gross, Francisco Massa, Adam Lerer, James Bradbury, Gregory Chanan, Trevor Killeen, Zeming Lin, Natalia Gimelshein, Luca Antiga, et al. 2019. Pytorch: An imperative style, high-performance deep learning library. *Advances in neural information processing systems* 32 (2019).
- [41] Fabian Pedregosa, Gaël Varoquaux, Alexandre Gramfort, Vincent Michel, Bertrand Thirion, Olivier Grisel, Mathieu Blondel, Peter Prettenhofer, Ron Weiss, Vincent Dubourg, et al. 2011. Scikit-learn: Machine learning in Python. *the Journal of machine Learning research* 12 (2011), 2825–2830.
- [42] Rafael Rafailov, Joey Hejna, Ryan Park, and Chelsea Finn. 2024. From \$r\$ to \$Q^\*\$: Your Language Model is Secretly a Q-Function. In *First Conference on Language Modeling*. <https://openreview.net/forum?id=kEVcNxtqXk>
- [43] Rafael Rafailov, Archit Sharma, Eric Mitchell, Christopher D Manning, Stefano Ermon, and Chelsea Finn. 2023. Direct preference optimization: Your language model is secretly a reward model. *Advances in Neural Information Processing Systems* 36 (2023), 53728–53741.
- [44] Lorenzo Rosasco, Ernesto De Vito, Andrea Caponnetto, Michele Piana, and Alessandro Verri. 2004. Are loss functions all the same? *Neural computation* 16, 5 (2004), 1063–1076.
- [45] Karan Sameil, Cheng Li, Weize Kong, Tao Chen, Mingyang Zhang, Shaleen Gupta, Swaraj Khadanga, Wensong Xu, Xingyu Wang, Kashyap Kolipaka, et al. 2023. End-to-End Query Term Weighting. In *Proceedings of the 29th ACM SIGKDD Conference on Knowledge Discovery and Data Mining*. 4778–4786.
- [46] Tao Shen, Xiubo Geng, Chongyang Tao, Can Xu, Guodong Long, Kai Zhang, and Daxin Jiang. 2023. Unifiter: A unified retriever for large-scale retrieval. In *Proceedings of the 29th ACM SIGKDD Conference on Knowledge Discovery and Data Mining*. 4787–4799.
- [47] Charlie Victor Snell, Jaehoon Lee, Kelvin Xu, and Aviral Kumar. 2025. Scaling LLM Test-Time Compute Optimally Can be More Effective than Scaling Parameters for Reasoning. In *The Thirteenth International Conference on Learning Representations*. <https://openreview.net/forum?id=4FWAwZid2n>
- [48] Hugo Touvron, Louis Martin, Kevin Stone, Peter Albert, Amjad Almahairi, Yasmine Babaci, Nikolay Bashlykov, Soumya Batra, Prajjwal Bhargava, Shruiti Bhosale, et al. 2023. Llama 2: Open foundation and fine-tuned chat models. *arXiv preprint arXiv:2307.09288* (2023).
- [49] Peiyi Wang, Lei Li, Zhihong Shao, Runxin Xu, Damai Dai, Yifei Li, Deli Chen, Yu Wu, and Zhifang Sui. 2024. Math-Shepherd: Verify and Reinforce LLMs Step-by-step without Human Annotations. In *Proceedings of the 62nd Annual Meeting of the Association for Computational Linguistics (Volume 1: Long Papers)*, Lun-Wei Ku, Andre Martins, and Vivek Srikumar (Eds.). Association for Computational Linguistics, Bangkok, Thailand, 9426–9439. <https://doi.org/10.18653/v1/2024.acl-long.510>
- [50] Jason Wei, Xuezhi Wang, Dale Schuurmans, Maarten Bosma, Fei Xia, Ed Chi, Quoc V Le, Denny Zhou, et al. 2022. Chain-of-thought prompting elicits reasoning in large language models. *Advances in neural information processing systems* 35 (2022), 24824–24837.
- [51] Svante Wold, Kim Esbensen, and Paul Geladi. 1987. Principal component analysis. *Chemometrics and intelligent laboratory systems* 2, 1-3 (1987), 37–52.
- [52] Thomas Wolf, Lysandre Debut, Victor Sanh, Julien Chaumond, Clement Delangue, Anthony Moi, Pierric Cistac, Tim Rault, Rémi Louf, Morgan Funtowicz, et al. 2019. Huggingface’s transformers: State-of-the-art natural language processing. *arXiv preprint arXiv:1910.03771* (2019).
- [53] Zhaomin Wu, Jizhou Guo, Junyi Hou, Bingsheng He, Lixin Fan, and Qiang Yang. 2024. Model-Based Differentially Private Knowledge Transfer for Large Language Models. *arXiv preprint arXiv:2410.10481* (2024).
- [54] Zhihui Xie, Jizhou Guo, Tong Yu, and Shuai Li. 2024. Calibrating Reasoning in Language Models with Internal Consistency. In *The Thirty-eighth Annual Conference on Neural Information Processing Systems*. <https://openreview.net/forum?id=udZKVMpF35>
- [55] Wei Xiong, Hanning Zhang, Nan Jiang, and Tong Zhang. 2024. An Implementation of Generative PRM. <https://github.com/RLHFlow/RLHF-Reward-Modeling>.
- [56] Shicheng Xu, Liang Pang, Huawei Shen, Xueqi Cheng, and Tat-Seng Chua. 2024. Search-in-the-chain: Interactively enhancing large language models with search for knowledge-intensive tasks. In *Proceedings of the ACM Web Conference 2024*. 1362–1373.
- [57] Yuan Yao, Lorenzo Rosasco, and Andrea Caponnetto. 2007. On early stopping in gradient descent learning. *Constructive approximation* 26, 2 (2007), 289–315.
- [58] Qifan Yu, Wei Chow, Zhongqi Yue, Kaihang Pan, Yang Wu, Xiaoyang Wan, Juncheng Li, Siliang Tang, Hanwang Zhang, and Yueting Zhuang. 2024. AnyEdit: Mastering Unified High-Quality Image Editing for Any Idea. *arXiv preprint arXiv:2411.15738* (2024).
- [59] Lifan Yuan, Ganqu Cui, Hanbin Wang, Ning Ding, Xingyao Wang, Boji Shan, Zeyuan Liu, Jia Deng, Huimin Chen, Ruobing Xie, Yankai Lin, Zhenghao Liu, Bowen Zhou, Hao Peng, Zhiyuan Liu, and Maosong Sun. 2025. Advancing LLM Reasoning Generalists with Preference Trees. In *The Thirteenth International Conference on Learning Representations*. <https://openreview.net/forum?id=2ea5TNVR0c>
- [60] Rowan Zellers, Ari Holtzman, Yonatan Bisk, Ali Farhadi, and Yejin Choi. 2019. HellaSwag: Can a Machine Really Finish Your Sentence?. In *Proceedings of the 57th Annual Meeting of the Association for Computational Linguistics*.
- [61] Anqi Zhang, Yulin Chen, Jane Pan, Chen Zhao, Aurojit Panda, Jinyang Li, and He He. 2025. Reasoning Models Know When They’re Right: Probing Hidden States for Self-Verification. *arXiv preprint arXiv:2504.05419* (2025).
- [62] Jing Zhang, Xiaokang Zhang, Daniel Zhang-Li, Jifan Yu, Zijun Yao, Zeyao Ma, Yiqi Xu, Haohua Wang, Xiaohan Zhang, Nianyi Lin, et al. 2023. Glm-dialog: Noise-tolerant pre-training for knowledge-grounded dialogue generation. In *Proceedings of the 29th ACM SIGKDD Conference on Knowledge Discovery and Data Mining*. 5564–5575.
- [63] Xiaoying Zhang, Jean-Francois Ton, Wei Shen, Hongning Wang, and Yang Liu. 2024. Mitigating Reward Overoptimization via Lightweight Uncertainty Estimation. *Advances in Neural Information Processing Systems* 37 (2024), 81717–81747.
- [64] Ruiwen Zhou, Yingxuan Yang, Muning Wen, Ying Wen, Wenhao Wang, Chunling Xi, Guoqiang Xu, Yong Yu, and Weinan Zhang. 2024. Trad: Enhancing llm agents with step-wise thought retrieval and aligned decision. In *Proceedings of the 47th International ACM SIGIR Conference on Research and Development in Information Retrieval*. 3–13.
- [65] Banghua Zhu, Evan Frick, Tianhao Wu, Hanlin Zhu, Karthik Ganesan, Wei-Lin Chiang, Jian Zhang, and Jiantao Jiao. 2024. Starling-7B: Improving Helpfulness and Harmlessness with RLAI. In *First Conference on Language Modeling*. <https://openreview.net/forum?id=GqDntYTTbk>
- [66] Andy Zou, Long Phan, Sarah Chen, James Campbell, Phillip Guo, Richard Ren, Alexander Pan, Xuwang Yin, Mantas Mazeika, Ann-Kathrin Dombrowski, et al. 2023. Representation engineering: A top-down approach to ai transparency. *arXiv preprint arXiv:2310.01405* (2023).

## Appendix Contents

A	Baseline Reward Models Description	11
B	Detailed Approach for Combining SWIFT with External Reward Models	11
C	Implementation Details	11
C.1	Hardware and Software	11
C.2	Details of the Preliminary Experiments	11
C.3	SWIFT Training Details	12
C.4	Generation Details	12
C.5	Evaluation Details / Method to identify correctness	13
C.6	Details on EurusRM-7B fine-tuning	13
D	Ablation Study	13
D.1	Impact of Loss Function	13
D.2	Ablation Study on the Gating Mechanism	14
E	Examples of SWIFT Scored Response	14
F	Additional Results	24

## A Baseline Reward Models Description

To provide further context for the baseline reward models used in our experiments, we present a brief overview and links to their respective Hugging Face Model Hub pages:

- **EurusRM-7B:** EurusRM-7B is a 7B parameter reward model trained on a mixture of UltraInteract [59], UltraFeedback [11], and UltraSafety datasets [18], with a focus on improving reasoning performance. EurusRM-7B stands out as the best 7B RM overall and achieves similar or better performance than much larger baselines. Particularly, it outperforms GPT-4 in certain tasks.
- **Skywork-Reward-Llama-3.1-8B-v0.2:** This 8B parameter reward model is built on the Llama-3 architecture [16] and trained on a curated dataset of 80K high-quality preference pairs. It excels at handling preferences in complex scenarios, including challenging preference pairs, and span various domains such as mathematics, coding, and safety. As of October 2024, Skywork-Reward-Llama-3.1-8B-v0.2 ranks first among 8B models.
- **Starling-RM-7B:** Starling-RM-7B is a reward model trained from Llama2-7B-Chat [48], following the method of training reward models in the instructGPT paper [39]. It is trained with the Nectar preference dataset [65], which is based on GPT-4’s preferences.
- **UltraRM-13B:** UltraRM is a reward model initialized by Llama2-13B [48] and fine-tuned on the UltraFeedback dataset [11]. It achieves state-of-the-art performance among open-source reward models on public preference test sets.
- **RLHFlowRM-8B-Deepseek:** RLHFlowRM-8B-Deepseek is trained from Llama-3.1-8B-Instruct on Deepseek generated data. It is evaluated on GSM8K and MATH dataset and demonstrated significant performance gains.
- **Math-Shepherd-7B:** Math-Shepherd is trained with automatic process annotation. It is benchmarked on GSM8K and MATH dataset and substantially boosted the task-performing LLM’s performance.

## B Detailed Approach for Combining SWIFT with External Reward Models

In the Best-of-N (BoN) setting, we explore two strategies for combining the SWIFT reward ( $R_{SWIFT}$ ) with an external reward signal ( $R_{ext}$ ), typically from a traditional reward model. We have  $N$  reasoning paths.

- (1) **Ranking-based Combination:** Let  $rank_{SWIFT}(i)$  and  $rank_{ext}(i)$  be the ranks of the  $i$ -th reasoning path according to SWIFT and the external reward model, respectively (lower rank is better). The relative rank is:

$$rank_{rel}(i) = \max(rank_{SWIFT}(i), rank_{ext}(i)) \quad (6)$$

We select the path with the *lowest* relative rank:

$$i^* = \arg \min_{i \in \{1, \dots, N\}} rank_{rel}(i) \quad (7)$$

- (2) **Scaling-based Combination:** We linearly scale both rewards to the range  $[0, 1]$  for the  $N$  paths<sup>1</sup>:

$$\tilde{R}_{SWIFT}(i) = \frac{R_{SWIFT}(i) - \min_j R_{SWIFT}(j)}{\max_j R_{SWIFT}(j) - \min_j R_{SWIFT}(j)} \quad (8)$$

$$\tilde{R}_{ext}(i) = \frac{R_{ext}(i) - \min_j R_{ext}(j)}{\max_j R_{ext}(j) - \min_j R_{ext}(j)} \quad (9)$$

The aggregated reward is:

$$R_{agg}(i) = \frac{\tilde{R}_{SWIFT}(i) + \tilde{R}_{ext}(i)}{2} \quad (10)$$

We select the path with the highest combined reward:

$$i^* = \arg \max_{i \in \{1, \dots, N\}} R_{agg}(i) \quad (11)$$

These combination strategies allow us to leverage both internal (SWIFT) and external reward signals.

## C Implementation Details

This appendix provides additional details on the experimental setup and training procedures used in our work.

### C.1 Hardware and Software

We conduct our experiment in a system with 8x NVIDIA A100 GPUs (80GB each) and an Intel(R) Xeon(R) Gold 6346 CPU @ 3.10GHz with 1.0TB of CPU memory (large CPU memory is unnecessary). We used the PyTorch framework [40] for implementing our models and training procedures.

### C.2 Details of the Preliminary Experiments

Our pipeline consists of the following steps:

- (1) **Hidden State Extraction:** We use the Llama-3.1-8B-Instruct model [16] and extract the hidden states  $h_t^l$  for each token  $t$  at each layer  $l$  during the generation of reasoning paths on the MATH dataset [21].

<sup>1</sup>If all the rewards are equal, we set them all to 1.0, but this is almost impossible in practice.

- (2) **Averaging:** For each reasoning path, we average the hidden states across all tokens within that path to obtain a single vector representation  $\bar{h}^\ell$  for each layer  $\ell$ .
- (3) **Dimensionality Reduction (PCA):** We apply Principal Component Analysis (PCA) [51] to reduce the dimensionality of  $\bar{h}^\ell$  to 50 dimensions. This step helps to mitigate overfitting that we observed with direct application of LDA.
- (4) **Classification (LDA):** We train a Linear Discriminant Analysis (LDA) classifier [4] on the reduced representations to predict whether the reasoning path is correct or incorrect.

The entire pipeline is *linear* to validate that hidden states of the reasoning paths encode a linear representation. The PCA+LDA model was trained using the scikit-learn library [41]. We adopted the default settings in scikit-learn.

### C.3 SWIFT Training Details

The SWIFT model was trained using the AdamW optimizer [31] with the following hyperparameters:

- **Learning Rate:**  $1 \times 10^{-4}$
- **Weight Decay:**  $1 \times 10^{-5}$
- **Batch Size:** 16

For each dataset, we created a training set of 6000 instances, drawn from the original training set, and a held-out test set of 500 instances, drawn from the original validation set (due to the absence of labels in some datasets' test sets). This consistent data preparation approach was applied across all datasets, with the exceptions of GSM8K (where the original test set was used due to the lack of a validation set) and Imbue Code Comprehension (where we performed a manual train/test split as no split was provided).

In addition, we need to generate reasoning path and determine whether each reasoning path is correct. The generation details are provided in Appendix C.4 and the method of determining each reasoning path's correctness is detailed in Appendix C.5.

We employed early stopping [57] to prevent overfitting. We further split the training data into training and validation sets using an 80/20 ratio. After each training epoch, we evaluated the model's performance on the validation set. We used the cross-entropy with logits loss on validation set as the criterion for early stopping. We used a patience of 3 epochs, meaning that training was terminated if the validation loss did not improve for 3 consecutive epochs. The model with the lowest validation loss across all epochs was selected as the final SWIFT model.

### C.4 Generation Details

For generating reasoning paths, we employed bfloat16 precision [6] to accelerate inference and reduce memory consumption, using vLLM library [25] and Huggingface's transformers library [52]. For each of the 6000 training instances, we generated 8 reasoning paths (rollouts), with `max_new_tokens` to be 1024. We set temperature to be 1.0, but set `top_p` to be 0.9 to prevent generating garbage text. The input format strictly followed the **instruction-question** template:

```
[Dataset-specific Instruction]
[Question from Dataset]
```

Each dataset employed a fixed instruction template to ensure task alignment:

- **Math/GSM8K:**

```
Solve the following math problem
step-by-step.
Simplify your answer as much
as possible. Present your final
answer as \boxed{Your Answer}.
```

- **AQuA\_RAT:**

```
You are given a multiple-choice
question with five options (A-E).
Solve it step by step, then
present only one letter (A-E) in
the form \boxed{Letter}.
Remember to output \boxed{Letter}
at the end of your answer or it
will be considered incorrect.
```

- **Imbue Code Comprehension:**

```
Analyze the following problem
step-by-step. The question
includes a list of choices.
Select the most appropriate choice
from the provided options and
output your final answer enclosed
within \boxed{...},
ensuring that the content inside
\boxed{...} is valid Python
literal syntax.
```

- **HellaSwag:**

```
You are given a context and four
possible continuations (A-D).
Decide which option best continues
the context.
Explain your reasoning step by
step, then present only one letter
(A-D) in the form \boxed{Letter}.
Remember to output \boxed{Letter}
at the end of your answer or it
will be considered incorrect.
```

- **CoinFlip:**

Answer the following Boolean question with detailed reasoning. Explain your reasoning step-by-step and conclude with a final answer as `\boxed{Yes}` or `\boxed{No}`.

## C.5 Evaluation Details / Method to identify correctness

This section details how we determine each reasoning path’s correctness for both training and evaluation, and the method for FLOPs calculation.

Due to the potential for equivalent but syntactically different answers (e.g., "6/5" and "1.2"), a simple string comparison is insufficient for determining correctness in the MATH and GSM8K datasets. Therefore, we adopted a more sophisticated evaluation approach, leveraging the implementation from the code repository of Yuan et al. [59]. For the AQuA\_RAT, HellaSwag and CoinFlip dataset, although the output is a single letter, we also employ this approach for consistency. This implementation allows for the robust comparison of mathematical expressions, treating semantically equivalent answers as correct.

For the Imbue Code Comprehension dataset, to extract the model’s answer, we first searched for content within `\boxed{ }`. If no answer was found within this delimiter, we then attempted to extract the answer following the phrases below (case-insensitive):

- answer is
- answer:
- output is
- output:

As a final resort, if neither of the above methods yielded an answer, we used the entire model output as the extracted answer.

Recognizing that the task-performing model’s output format may be inconsistent, we implemented the following answer cleansing procedures:

- Removed any occurrences of `\text{...}` by replacing them with the inner text.
- Replaced escaped braces `\{` and `\}` with regular braces `{` and `}`.
- Remove Markdown code fences (````python` or `````) if present.
- Removed any extraneous whitespace.

Following answer extraction, we employed Python’s `ast.literal_eval` function to parse both the model’s output and the reference answer, and subsequently compared the parsed values. In cases where parsing failed, we implemented a fallback mechanism: treating the extracted content as a string, removing any surrounding quotes, and then comparing it with the reference answer (also stripped of surrounding quotes).

We use the Flops Profiler of DeepSpeed library [2] for FLOPs calculation.

## C.6 Details on EurusRM-7B fine-tuning

As a baseline to validate the superior performance of our SWIFT method, we fine-tuned the EurusRM-7B reward model [59] to provide a more comprehensive comparison, although it has already been pretrained on MATH and GSM8K dataset, which may give it a potential advantage. To ensure a fair comparison and control for data variance, we used an identical training dataset to that of SWIFT, consisting of 6,000 samples, each with 8 rollouts. Due to resource constraints, we employed Low-Rank Adaptation (LoRA) [22] for efficient fine-tuning. The AdamW optimizer was used with the following hyperparameters:

- **Learning Rate:**  $1 \times 10^{-5}$
- **Weight Decay:**  $1 \times 10^{-5}$
- **Batch Size:** 1

Our fine-tuning process employs a loss function identical to that of the original paper Yuan et al. [59]. The specific loss function,  $\mathcal{L}_{\text{ULTRAINTERACT}}$ , is defined as follows:

$$\mathcal{L}_{\text{ULTRAINTERACT}} = \underbrace{-\log(\sigma(r_{\theta}(x, y_c) - r_{\theta}(x, y_r)))}_{\mathcal{L}_{\text{BT}}: \text{optimize relative rewards}} - \underbrace{\log(\sigma(r_{\theta}(x, y_c))) - \log(\sigma(-r_{\theta}(x, y_r)))}_{\mathcal{L}_{\text{DR}}: \text{increase } r_{\theta}(x, y_c) \text{ and decrease } r_{\theta}(x, y_r)} \quad (12)$$

In this formulation,  $x$  denotes the problem prompt,  $y_c$  represents the chosen (correct) answer, and  $y_r$  is the rejected (incorrect) answer. The reward model, parameterized by  $\theta$ , is denoted by  $r_{\theta}(\cdot)$ , and  $\sigma$  is the sigmoid function. The  $\mathcal{L}_{\text{BT}}$  term is a Bradley-Terry-style loss that optimizes the relative rewards, encouraging the reward of the correct answer to be higher than that of the incorrect one. The  $\mathcal{L}_{\text{DR}}$  term directly regularizes the rewards by increasing the reward for the chosen answer and decreasing it for the rejected answer.

Furthermore, our data sampling methodology is analogous to the approach described in the original paper. For each problem instance, a training pair is constructed by randomly matching one correct solution with one incorrect solution from the same problem.

We report the results for fine-tuning Eurus-7B on each LLM’s generated reasoning path of each dataset, to ensure a fair comparison. The model is fine-tuned for 4 epochs. The LoRA configuration was set to `lora_r=4` and `lora_alpha=8`. The `lora_r` parameter defines the rank of these adaptation matrices, controlling the dimensionality of the update. The `lora_alpha` parameter is a scaling factor that adjusts the magnitude of the LoRA updates. The actual update is scaled by  $\frac{\text{lora\_alpha}}{\text{lora\_r}}$ .

## D Ablation Study

### D.1 Impact of Loss Function

This section investigates the impact of different loss functions on the performance of the SWIFT model. We compare our chosen cross-entropy with logits loss with hinge loss, Direct Preference Optimization (DPO) loss, InfoNCA loss, and NCA loss.

#### D.1.1 Loss Function Formulations.

- Cross-Entropy with Logits Loss [42]: Given a binary label  $y \in \{0, 1\}$  (where 1 represents a correct path and 0 an incorrect

path) and a predicted reward  $R$ , the CE loss with logits is:

$$\mathcal{L}_{CE} = -[y \log(\sigma(R)) + (1 - y) \log(1 - \sigma(R))] \quad (13)$$

where  $\sigma(x) = \frac{1}{1+e^{-x}}$  is the sigmoid function.

- Hinge Loss [44]: As defined in Section 4.2, the hinge loss for a reasoning path with a predicted reward  $R$  is:

$$\mathcal{L}_{hinge} = \max(0, 1 - y \cdot R) \quad (14)$$

- Direct Preference Optimization (DPO) Loss [43]: Given the reward for a positive (chosen) path  $r^+$  and the reward for a negative (rejected) path  $r^-$ , the DPO loss is:

$$\mathcal{L}_{DPO} = -\log(\sigma(r^+ - r^-)) \quad (15)$$

where  $\sigma(x)$  is the sigmoid function.

- InfoNCA Loss [9]: Given predicted rewards  $r_{pred} \in \mathbb{R}^K$  for  $K$  candidate paths and corresponding ground-truth rewards  $r_{gt} \in \mathbb{R}^K$ , and a temperature parameter  $\alpha$ , the InfoNCA loss is:

$$\mathcal{L}_{InfoNCA} = -\sum_{i=1}^K \left[ \text{softmax}\left(\frac{r_{gt}}{\alpha}\right)_i \cdot \log\left(\text{softmax}(r_{pred})_i\right) \right] \quad (16)$$

- NCA Loss [9]: With the same notation as InfoNCA, the NCA loss is:

$$\mathcal{L}_{NCA} = -\sum_{i=1}^K \left[ \text{softmax}\left(\frac{r_{gt}}{\alpha}\right)_i \cdot \log(\sigma(r_{pred}_i)) + \frac{1}{K} \log(\sigma(-r_{pred}_i)) \right] \quad (17)$$

**D.1.2 Experimental Results.** We train the SWIFT model using each of these loss functions, keeping all other hyperparameters constant (as detailed in Appendix A). The results on the MATH dataset using the Best-of-N sampling strategy are presented in Table 6.

For InfoNCA and NCA, we set the temperature  $\alpha = 0.01$ . Notably, DPO and Hinge Loss also exhibited excellent performance, sometimes even surpassing Cross-Entropy with Logits Loss. Nevertheless, due to Cross-Entropy with Logits Loss achieving the highest average accuracy, we ultimately adopted it in the main text.

## D.2 Ablation Study on the Gating Mechanism

To assess the necessity of the gating mechanism within our SWIFT framework, we conducted an ablation study on the MATH dataset. We compared the performance of SWIFT with and without the gating mechanism across three different models: Llama-3-3B, Llama-3-8B, and Ministral-8B. The results are summarized in Table 7.

The results indicate that while SWIFT without the gating mechanism can achieve reasonable performance, it consistently underperforms SWIFT with the gating mechanism across all models and  $k$  values. This suggests that the gating mechanism plays a crucial role in improving reasoning accuracy.

## E Examples of SWIFT Scored Response

We provide specific examples of SWIFT scores for LLM reasoning paths in Table 8. We highlight the top and bottom 10 tokens based on their SWIFT gating  $\times$  reward values, while also preserving special tokens such as `<|eot_id|>` (end-of-turn identifier). The 10 tokens with the highest gating  $\times$  reward are highlighted in **limegreen** (approximating green), while the 10 tokens with the lowest gating

$\times$  reward are highlighted in **salmon** (approximating red). Each highlighted token is also annotated with its corresponding gating  $\times$  reward value. For each dataset and task-performing LLM, we provide one example, including whether the reasoning path is correct or incorrect, and the final reward assigned by SWIFT.

Table 8 presents nine examples of SWIFT’s scored reasoning paths. Notably, SWIFT’s gating  $\times$  reward scores demonstrate sensitivity to specific elements within the reasoning sequence, tending to assign high scores (highlighted in **limegreen**) to numerical and mathematical symbols, as well as tokens like “answer”, “boxed”, and the special token `<|eot_id|>` when the overall reward is positive, and low scores (highlighted in **salmon**) to these same kinds of tokens when the overall reward is negative. This pattern suggests that SWIFT is capable of discerning and prioritizing salient aspects of the reasoning process, weighting these key tokens positively when the reasoning leads to a correct answer and negatively otherwise.

**Table 6: Comparison of different loss functions for training SWIFT on the MATH dataset. Bold: best performance; Underline: second-best performance.**

MATH Dataset										
Type	Llama-3.2-3B			Llama-3.1-8B			Ministral-8B			Avg.
	@4	@16	@64	@4	@16	@64	@4	@16	@64	
Hinge Loss	47.8	53.4	53.0	55.2	<u>58.4</u>	57.8	<b>58.0</b>	<b>62.6</b>	<b>64.6</b>	56.8
DPO	<u>49.0</u>	<b>55.4</b>	<b>55.4</b>	<b>55.4</b>	56.8	<u>58.2</u>	<b>58.0</b>	<b>62.6</b>	62.0	<u>57.0</u>
InfoNCA ( $\alpha = 0.01$ )	47.8	52.2	49.0	54.8	55.6	55.8	57.6	61.0	62.2	55.1
NCA ( $\alpha = 0.01$ )	46.8	50.8	49.8	54.0	55.2	54.2	<b>58.0</b>	59.4	61.8	54.4
Cross-Entropy	<b>49.8</b>	<u>54.6</u>	<u>53.6</u>	<b>55.4</b>	<b>59.4</b>	<b>62.6</b>	57.8	61.6	<u>62.8</u>	<b>57.5</b>

**Table 7: Ablation Study on the Gating Mechanism on the MATH Dataset. Bold: best performance;**

MATH Dataset										
Type	Llama-3.2-3B			Llama-3.1-8B			Ministral-8B			Avg.
	@4	@16	@64	@4	@16	@64	@4	@16	@64	
Without Gating	46.8	50.2	49.4	54.2	56.2	57.6	56.6	60.4	61.4	54.8
With Gating	<b>49.8</b>	<b>54.6</b>	<b>53.6</b>	<b>55.4</b>	<b>59.4</b>	<b>62.6</b>	<b>57.8</b>	<b>61.6</b>	<b>62.8</b>	<b>57.5</b>

**Table 8: Examples of SWIFT Score Reasoning Paths.** The 10 tokens with the highest gating  $\times$  reward are highlighted in limegreen, while the 10 tokens with the lowest gating  $\times$  reward are highlighted in salmon. Each highlighted token is also annotated with its corresponding gating  $\times$  reward value. Special tokens such as `<|eot_id|>` (end-of-turn identifier) are preserved.

Example 1	
<b>Dataset</b>	MATH
<b>Task-performing LLM</b>	Llama-3.2-3B
<b>Question</b>	If $f(x) = \frac{3x-2}{x-2}$ , what is the value of $f(-2) + f(-1) + f(0)$ ? Express your answer as a common fraction.
<b>Response</b>	<p>Step 1: We need to find the values of <math>f(-2)</math>, <math>f(-1)</math>, and <math>f(0)</math> by substituting the corresponding values of <math>x</math> into the function <math>f(x) = \frac{3x-2}{x-2}</math>.</p> <p>Step 2: Calculate the value of <math>f(-2)</math>. Substitute <math>x = -2</math> into the function: <math>f(-2) = \frac{3(-2) - 2}{-2 - 2} = \frac{-6 - 2}{-4} = \frac{-8}{-4} = 2</math></p> <p>Step 3: Calculate the value of <math>f(-1)</math>. Substitute <math>x = -1</math> into the function: <math>f(-1) = \frac{3(-1) - 2}{-1 - 2} = \frac{-3 - 2}{-3} = \frac{-5}{-3} = \frac{5}{3}</math></p> <p>Step 4: Calculate the value of <math>f(0)</math>. Substitute <math>x = 0</math> into the function: <math>f(0) = \frac{3(0) - 2}{0 - 2} = \frac{-2}{-2} = 1</math></p> <p>Step 5: Add the values of <math>f(-2)</math>, <math>f(-1)</math>, and <math>f(0)</math>: <math>f(-2) + f(-1) + f(0) = 2 + \frac{5}{3} + 1 = \frac{6}{3} + \frac{5}{3} + \frac{3}{3} = \frac{14}{3}</math></p> <p><b>Answer:</b> <math>\boxed{\frac{14}{3}}</math></p>
<b>Final Reward</b>	5.11
<b>Correctness</b>	True
<b>Reference Answer</b>	$\frac{14}{3}$

Example 2

<b>Dataset</b>	MATH
<b>Task-performing LLM</b>	Llama-3.1-8B
<b>Question</b>	<p>Let <math>a</math> be a positive real number such that all the roots of</p> $x^3 + ax^2 + ax + 1 = 0$ <p>are real. Find the smallest possible value of <math>a</math>.</p>
<b>Response</b>	<pre> Step 1: Problem Explanation We are given a cubic equation <math>x^3 + ax^2 + ax + 1 = 0</math> and asked to find the smallest possible value of <math>a</math> such that all the roots of the equation are real. Step 2: To approach this problem, we will use Vieta's formulas, which relate the coefficients of a polynomial to sums and products of its roots. For a cubic equation of the form <math>x^3 + bx^2 + cx + d = 0</math> with roots <math>r, s, t</math>, Vieta's formulas state that <math>r + s + t = -b</math>, <math>rs + st + tr = c</math>, and <math>rst = -d</math>. python import math # define the function to calculate the value of a def calculate_a(): # Calculate the discriminant of the equation # For the roots to be real, the discriminant must be non-negative # The discriminant of the cubic equation is <math>b^2 * c^2 - 4 * a * d</math> # In this case, <math>b = a, c = a, d = 1</math> # So, we have <math>a^2 * a^2 - 4 * a * 1 \geq 0</math> # This simplifies to <math>a^4 - 4a \geq 0</math> # To find the smallest possible value of <math>a</math>, we need to find the minimum of the expression <math>a^4 - 4a</math> # We can do this by finding the critical points of the function <math>f(a) = a^4 - 4a</math> # Taking the derivative of <math>f(a)</math> with respect to <math>a</math>, we get <math>f'(a) = 4a^3 - 4</math> # Setting <math>f'(a) = 0</math>, we get <math>4a^3 - 4 = 0</math> # Solving for <math>a</math>, we get <math>a^3 = 1</math> # Taking the square root of both sides, we get <math>a = \pm \sqrt[3]{1}</math> # Since <math>a</math> is a positive real number, the smallest possible value of <math>a</math> is <math>\sqrt[3]{1}</math> a = 2/math.sqrt(3) return a result = calculate_a() print("The final answer is \boxed{\frac{2}{\sqrt{3}}}") &lt;leot_id&gt; </pre>
<b>Final Reward</b>	-7.41
<b>Correctness</b>	False
<b>Reference Answer</b>	3

Example 3

<b>Dataset</b>	MATH
<b>Task-performing LLM</b>	Ministral-8B
<b>Question</b>	<p>The volume of the cylinder shown is <math>45\pi</math> cubic cm. What is the height in centimeters of the cylinder? [asy]</p> <pre>size(120); draw(shift(2.2,0)*yscale(0.3)*Circle((0,0), 1.2)); draw((1,0)–(1,-2)); draw((3.4,0)–(3.4,-2)); draw((1,-2)..(2.2,-2.36)..(3.4,-2)); label("h",midpoint((3.4,0)–(3.4,-2)),E); draw(((2.2,0)–(3.4,0))); label("r = 3",midpoint((2.2,0)–(3.4,0)),N); [/asy]</pre>
<b>Response</b>	<p>Given the volume of the cylinder is <math>45\pi</math> cubic cm and the radius <math>r = 3</math> cm, we can use the formula for the volume of a cylinder:</p> $V = \pi r^2 h$ <p>Substituting the given values:</p> $45\pi = \pi \cdot 3^2 \cdot h$ $45\pi = 9\pi h$ $h = \frac{45\pi}{9\pi}$ <p>Thus, the height of the cylinder is <math>5</math> cm.</p>
<b>Final Reward</b>	9.07
<b>Correctness</b>	True
<b>Reference Answer</b>	5

Example 4

<b>Dataset</b>	GSM8K
<b>Task-performing LLM</b>	Llama-3.2-3B
<b>Question</b>	A robe takes 2 bolts of blue fiber and half that much white fiber. How many bolts in total does it take?
<b>Response</b>	<p>To solve the problem, we first need to determine the amount of blue and white fiber required. Since it takes 2 bolts of blue fiber, we can start by writing that as 2. Let's denote the amount of white fiber as <math>x</math>. According to the problem, it takes half that much white fiber, so the equation for the total amount of fiber required would be:</p> $2 \text{ (blue)} + 0.5x \text{ (white)} = \text{total}$ <p>Since the problem doesn't specify the total amount of fiber, let's assume that we are looking for the total amount of fiber in terms of <math>x</math>. The total amount of fiber required is the sum of blue and white fibers, which is <math>2 + 0.5x</math>. Since we can't simplify this expression further, the solution is <math>2 + 0.5x</math>. However, to adhere to the requested answer format, the final answer should be presented in the box and include the value of <math>x</math>. In this case, since <math>x</math> is an unknown value and not a numerical one, it cannot be simplified to a single number, the solution is expressed in terms of <math>x</math>, <math>2 + 0.5x</math>, but it is not exactly fitting the requested answer format, that being a simple answer in a box. Since it does not specify the value of <math>x</math>, it cannot be simplified further in terms of a single number. But since it is required to follow the format to the letter the answer is: <math>\boxed{2 + 0.5x}</math></p>
<b>Final Reward</b>	-5.54
<b>Correctness</b>	False
<b>Reference Answer</b>	3

Example 5

<b>Dataset</b>	GSM8K
<b>Task-performing LLM</b>	Llama-3.1-8B
<b>Question</b>	Carla is downloading a 200 GB file. Normally she can download 2 GB/minute, but 40% of the way through the download, Windows forces a restart to install updates, which takes 20 minutes. Then Carla has to restart the download from the beginning. How long does it take to download the file?
<b>Response</b>	<p>To find the total download time, we need to calculate the time spent downloading the first 40% of the file, the time spent waiting for the update to install, and the time spent downloading the remaining 60% of the file.</p> <ol style="list-style-type: none"> <li>Find the time spent downloading the first 40% of the file:  <math>40\% \text{ of } 200 \text{ GB} = 0.4 * 200 = 80 \text{ GB}</math> Time spent downloading 80 GB at 2 GB/minute = <math>80 / 2 = 40</math> minutes</li> <li>Time spent waiting for the update to install = 20 minutes</li> <li>Find the time spent downloading the remaining 60% of the file :  <math>60\% \text{ of } 200 \text{ GB} = 0.6 * 200 = 120 \text{ GB}</math> Time spent downloading 120 GB at 2 GB / minute = <math>120 / 2 = 60</math> minutes</li> <li>Total time spent downloading the file = time spent downloading the first 40% + time spent waiting for the update + time spent downloading the remaining 60% Total time = <math>40 + 20 + 60 = 120</math> minutes The total time spent downloading the file is 120 minutes</li> </ol>
<b>Final Reward</b>	-7.14
<b>Correctness</b>	False
<b>Reference Answer</b>	160

Example 6

<b>Dataset</b>	GSM8K
<b>Task-performing LLM</b>	Ministral-8B
<b>Question</b>	Claire makes a 3 egg omelet every morning for breakfast. How many dozens of eggs will she eat in 4 weeks?
<b>Response</b>	<ol style="list-style-type: none"> <li>Determine the number of days in 4 weeks: <math>4 \text{ weeks} \times 7 \text{ days/week} = 28 \text{ days}</math></li> <li>Calculate the total number of eggs Claire eats in 4 weeks: <math>3 \text{ eggs/day} \times 28 \text{ days} = 84 \text{ eggs}</math></li> <li>Convert the total number of eggs to dozens (1 dozen = 12 eggs): <math>\frac{84 \text{ eggs}}{12 \text{ eggs/dozen}} = 7 \text{ dozens}</math> Therefore, Claire will eat 7 dozens of eggs in 4 weeks.</li> </ol>
<b>Final Reward</b>	12.23
<b>Correctness</b>	True
<b>Reference Answer</b>	7

Example 7

<b>Dataset</b>	AQuA_RAT
<b>Task-performing LLM</b>	Llama-3.2-3B
<b>Question</b>	A ship is leaving a port. It takes 240 seconds to pass through a 750m channel to get to the port gates, and takes 60 seconds to pass through the gates of the port. What is its length? A)100 m B)150 m C)200 m D)250 m E)300 m
<b>Response</b>	<p>To solve this problem, we need to use the concept of speed. The speed of the ship can be calculated by dividing the distance it travels by the time it takes. Let's break it down step by step:</p> <ol style="list-style-type: none"> <li>1. Time taken to pass through the channel = 240 seconds</li> <li>2. Distance traveled through the channel = 750 meters</li> <li>3. Speed of the ship = Distance / Time = 750 meters / 240 seconds = 3.125 meters per second</li> </ol> <p>Now, let's find the speed of the ship when passing through the gates of the port:</p> <ol style="list-style-type: none"> <li>4. Time taken to pass through the gates = 60 seconds</li> <li>5. Speed of the ship = Distance / Time = x meters / 60 seconds. Since the ship's speed is the same in both cases, we can set up an equation: <math>3.125 = x / 60</math></li> <li>7. To solve for x, we multiply both sides by 60: <math>x = 3.125 \times 60 = 187.5</math> meters. Since the ship is leaving the port, we need to add the length of the ship to the distance it traveled through the channel to get the total length. However, the question doesn't provide the length of the ship. But we can find the length by using the distance traveled through the gates: Total length of the ship = 187.5 meters. Since we're looking for a multiple-choice answer, we need to look at the options and find the closest match. The closest match is B) 150 m.</li> </ol>
<b>Final Reward</b>	-9.48
<b>Correctness</b>	False
<b>Reference Answer</b>	D



Example 9

<b>Dataset</b>	AQuA_RAT
<b>Task-performing LLM</b>	Ministral-8B
<b>Question</b>	A rectangular piece of cloth 2 feet wide was cut lengthwise into two smaller rectangular pieces. The shorter piece was one-third of the length of the longer of the 2 new pieces and had an area of 12 square feet. What was the length Q in feet of the original piece of cloth before cutting? A)6 B)18 C)24 D)36 E)48
<b>Response</b>	<p>1. Let <math>(l)</math> be the length of the longer piece and <math>(w)</math> be the width of the original piece. The shorter piece is <math>(\frac{1}{3}l)</math>.</p> <p>2. Given the width of the original piece is 2 feet, the shorter piece's dimensions are <math>(\frac{1}{3}l \times 2)</math>.</p> <p>3. The area of the shorter piece is given by: <math>(2 \times \frac{1}{3}l = 12 \text{ square feet})</math></p> <p>4. Solving for <math>(l)</math>: <math>(\frac{2l}{3} = 12 \implies 2l = 18 \implies l = 9 \text{ feet})</math></p> <p>5. The longer piece has a length <math>(l = 9)</math> feet, and the shorter piece has a length <math>(\frac{1}{3}l = 3)</math> feet.</p> <p>6. The original piece had a total length <math>(l + \frac{1}{3}l)</math>: <math>(9 + 3 = 12 \text{ feet})</math> Therefore, the length <math>(Q)</math> of the original piece of cloth is <math>(12)</math> feet.</p>
<b>Final Reward</b>	-8.57
<b>Correctness</b>	False
<b>Reference Answer</b>	C

## **F Additional Results**

Received 20 February 2007; revised 12 March 2009; accepted 5 June 2009

This section provides additional results of our experiments. Please refer to the next page.

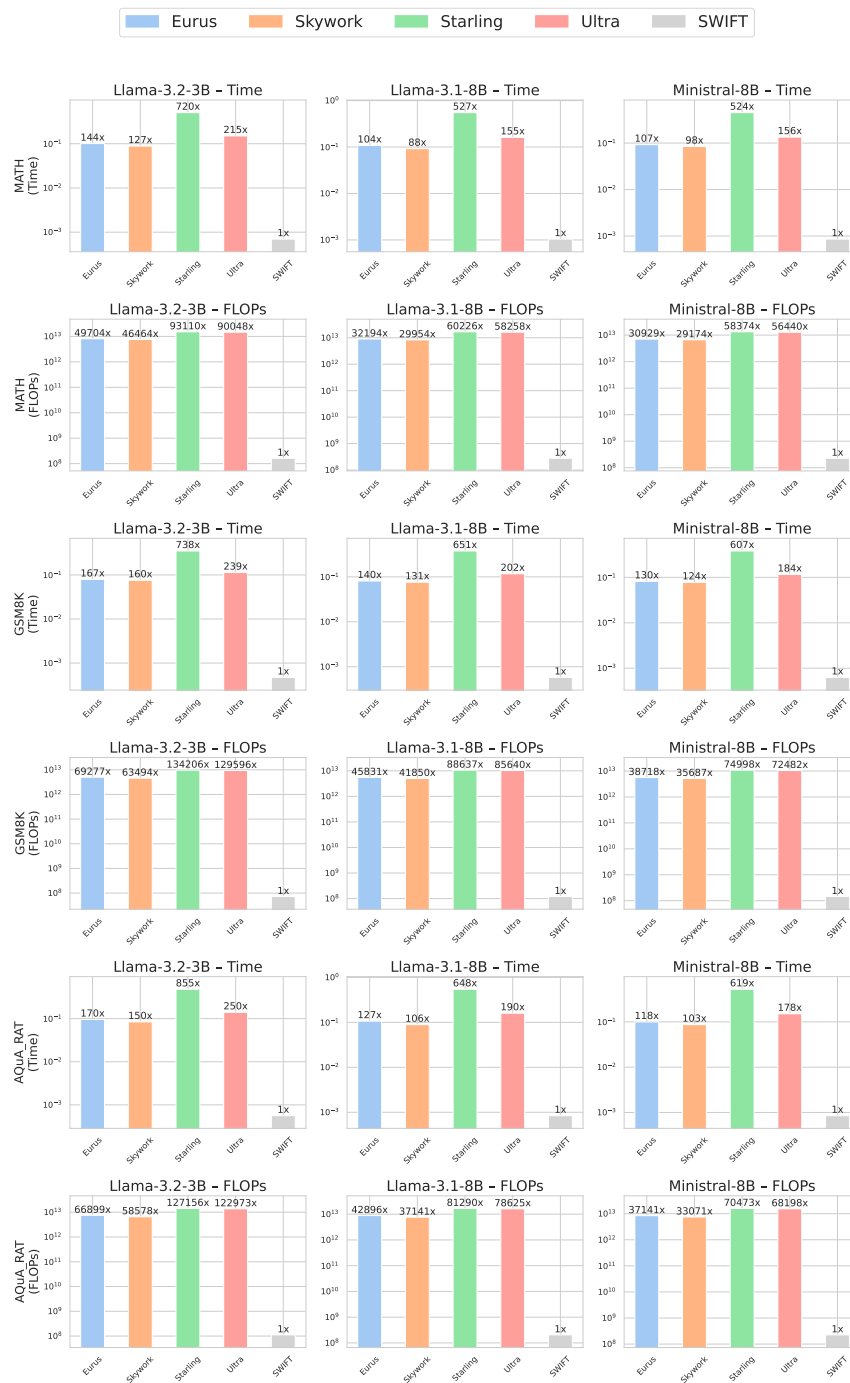


**Figure 6: Comparison of average time and FLOPs per sample for the proposed SWIFT reward model and baseline reward models, evaluated on different datasets and task-performing models. The y-axis is plotted in log-scale. The results show that SWIFT achieves orders-of-magnitude higher efficiency than the baselines.**

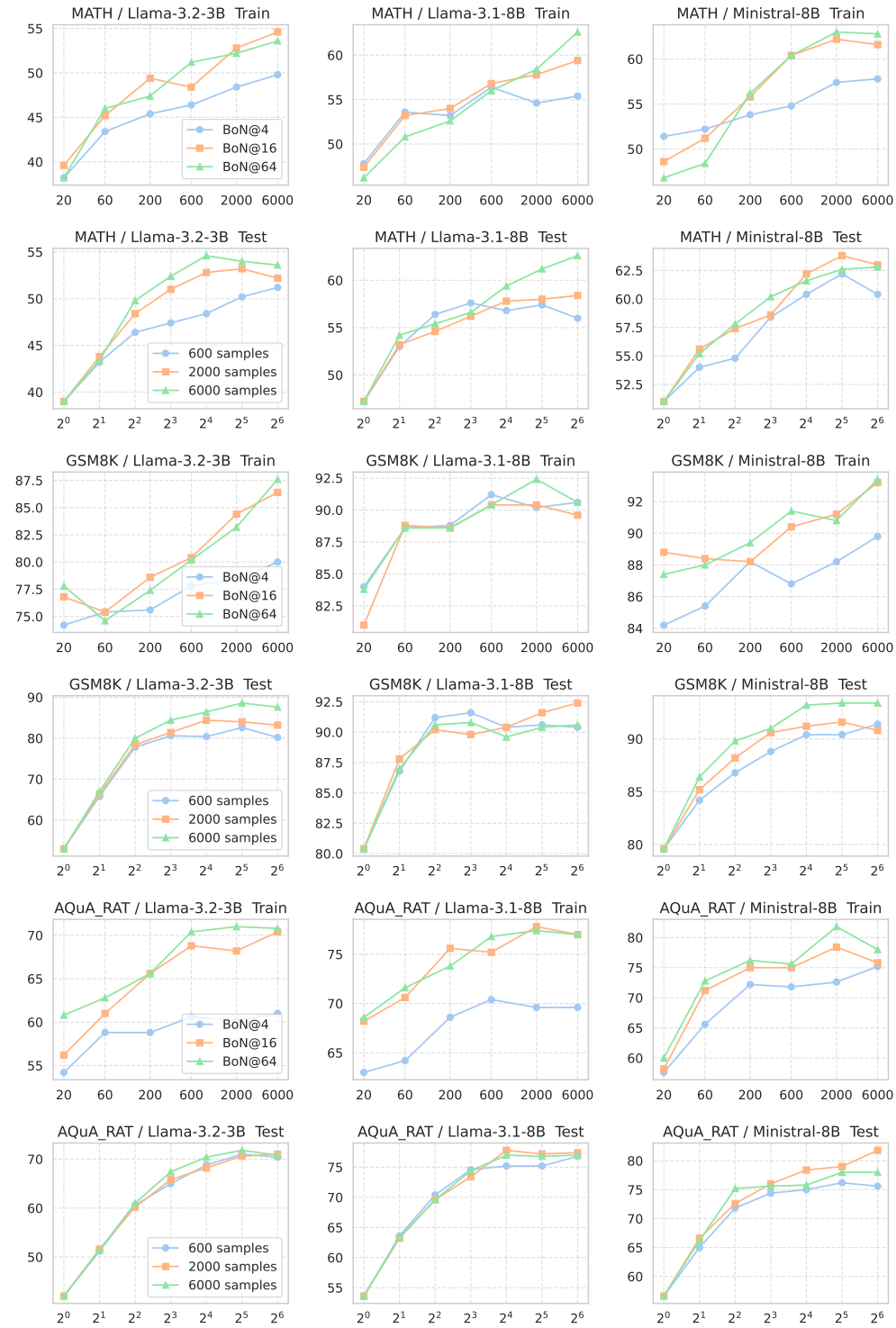
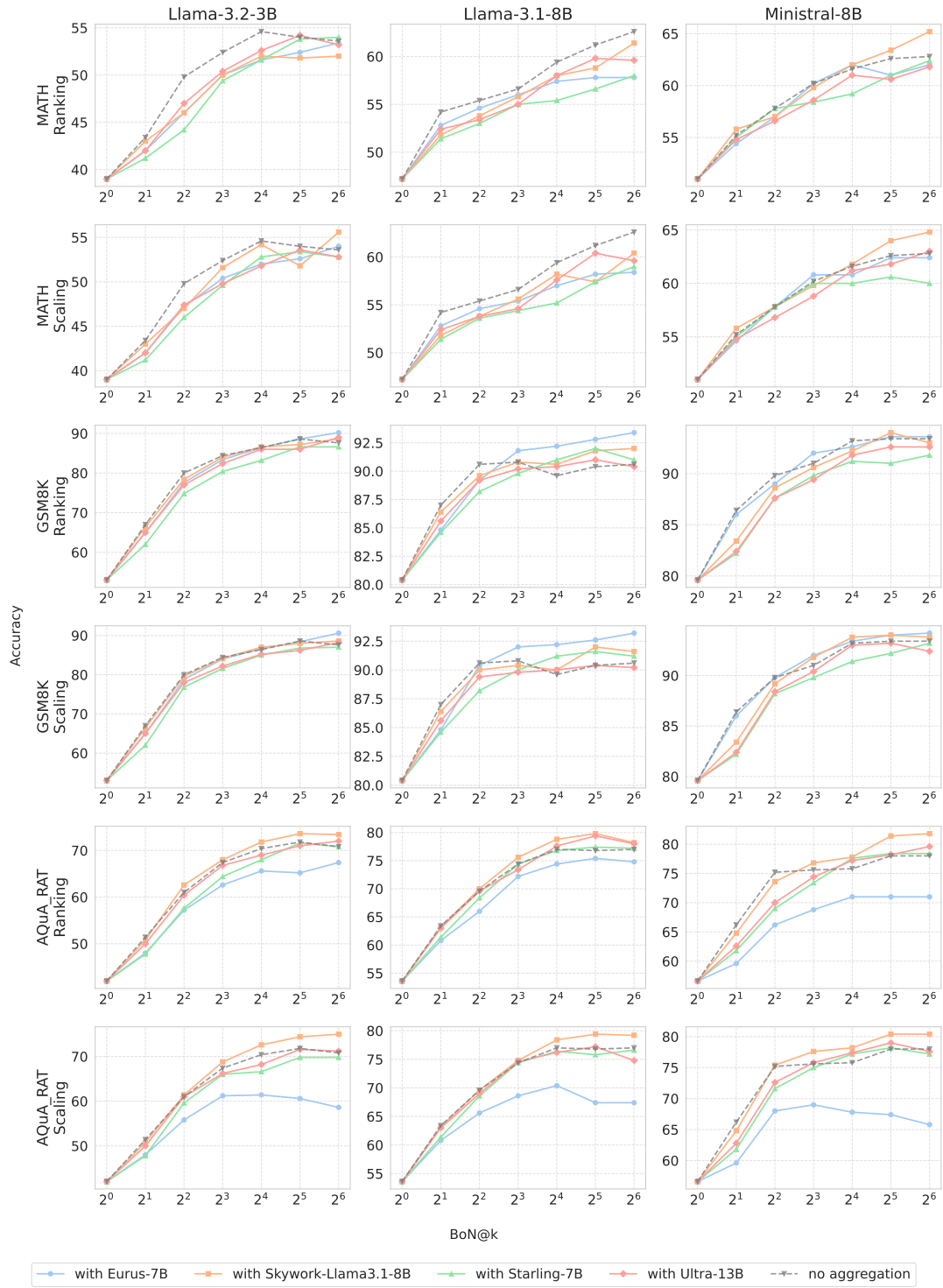


Figure 7: SWIFT has positive scaling with increased number of training samples and with the number of reasoning paths for inference.



**Figure 8: Performance of combined SWIFT and external reward models across different datasets and task-performing models, using both rank selection and scaled averaging.**

**Table 9: Training SWIFT solely on logits can also yield high performance and can outperform many baselines with orders-of-magnitude higher efficiency.**

MATH Dataset										
Method	Llama-3.2-3B BoN@1: 39.0			Llama-3.1-8B BoN@1: 47.2			Ministral-8B BoN@1: 51.0			Avg.
	@4	@16	@64	@4	@16	@64	@4	@16	@64	
SWIFT on logits	44.6	49.6	50.6	54.2	54.4	55.8	53.4	55.6	57.4	52.8
GSM8K Dataset										
Method	Llama-3.2-3B BoN@1: 39.0			Llama-3.1-8B BoN@1: 47.2			Ministral-8B BoN@1: 51.0			Avg.
	@4	@16	@64	@4	@16	@64	@4	@16	@64	
SWIFT on logits	76.0	79.6	81.0	89.2	90.6	91.2	87.4	87.0	90.2	85.8
AQuA_RAT Dataset										
Method	Llama-3.2-3B BoN@1: 39.0			Llama-3.1-8B BoN@1: 47.2			Ministral-8B BoN@1: 51.0			Avg.
	@4	@16	@64	@4	@16	@64	@4	@16	@64	
SWIFT on logits	58.8	63.4	65.2	68.6	77.2	78.0	69.6	74.4	74.0	69.9